The climatic debt is growing in the understorey of temperate forests: Stand characteristics matter

Benoit Richard, Jean-luc Dupouey, Emmanuel Corcket, Didier Alard, Frédéric Archaux, Michaël Aubert, Vincent Boulanger, François Gillet, Estelle Langlois, Sébastien Macé, et al.

The climatic debt is growing in the understory of temperate forests: stand characteristics matter

Running title:

- Explaining the climatic debt of temperate forests

Authors

Benoit Richard[1,2] | Jean-Luc Dupouey[3] | Emmanuel Corcket[4] | Didier Alard[4] | Frédéric Archaux[5] | Michaël Aubert[2] | Vincent Boulanger[6] | François Gillet[7] | Estelle Langlois[2] | Sébastien Macé[6] | Pierre Montpied[3] | Thérèse Beaufils[7] | Carole Begeot[7] | Patrick Behr[3] | Jean-Michel Boissier[8] | Sylvaine Camaret[9] | Richard Chevalier[5] | Guillaume Decocq[1] | Yann Dumas[5] | Richard Eynard-Machet[10] | Jean-Claude Gégout[3] | Sandrine Huet[11] | Valéry Malécot[11] | Pierre Margerie[2] | Arnaud Mouly[7] | Thierry Paul[3] | Benoît Renaux[12] | Pascale Ruffaldi[7] | Fabien Spicher[1] | Erwin Thirion[3] | Erwin Ulrich[6] | Manuel Nicolas[6] | Jonathan Lenoir[1*]

Authors' affiliations

[1]UMR CNRS 7058 « Ecologie et Dynamique des Systèmes Anthropisés » (EDYSAN), Université de Picardie Jules Verne, Amiens, France

[2]Normandie Université, UNIROUEN, INRAE, ECODIV, Rouen, France

[3]Université de Lorraine, AgroParisTech, INRAE, SILVA, Nancy, France

[4]Université de Bordeaux, INRAE, BIOGECO, Pessac, France

[5]INRAE, UR EFNO, Domaine des Barres, Nogent-sur-Vernisson, France

[6]Office National des Forêts, Département RDI, Fontainebleau, France

[7]UMR CNRS 6249 Chrono-Environnement, Université Bourgogne Franche-Comté, Besançon, France

[8]Ecosylve, Les Déserts, France

[9]UFR LLSH, Université Savoie Mont Blanc, Domaine Universitaire de Jacob-Bellecombette, Chambéry, France

[10]e-Sciences, Cognin, France

[11]Agrocampus-Ouest, INRAE, Université d'Angers, IRHS, Beaucouzé, France

[12]Conservatoire botanique national du Massif central, Chavaniac-Lafayette, France

*jonathan.lenoir@u-picardie.fr

The climatic debt is growing in the understory of temperate forests: stand characteristics matter

Running title:

- Explaining the climatic debt of temperate forests

Abstract

Aim

Climate warming reshuffles biological assemblages towards less cold-adapted but more warm-adapted species, a process coined thermophilization. However, the velocity at which this process happens is generally lagging behind the velocity of climate change, generating a climatic debt which temporal dynamic remains misunderstood. Relying on high-resolution time series of vegetation data from a long-term monitoring network of permanent forest plots, we aim at quantifying the temporal dynamic – up to a yearly resolution – of the climatic debt in the understory of temperate forests before identifying the key determinants allowing to modulate it.

Location

France

Time period

1995-2017

Taxa studied

Vascular plants

Methods

We used the community temperature index (CTI) to produce a time series of understory plant community thermophilization, which we subsequently compared to a time series of mean annual temperature changes over the same period and for the same sites. The direction and magnitude of the difference (i.e. the climatic debt) was finally analyzed using linear mixed-effect models to assess the relative contribution of abiotic and biotic determinants, including forest stand characteristics.

Results

We found a significant increase in CTI values over time (0.08–0.09°C/decade), whereas the velocity of mean annual temperature changes was three times higher over the same period (0.22–0.28°C/decade). Hence, the climatic debt increased over time and was greater in forest stands with higher basal area or older trees as well as under warmer macroclimate. By contrasts, a greater frequency of anthropogenic disturbances decreased the climatic debt, while natural disturbances and herbivory had no impact.

Conclusions

Although often overlooked in understanding the climatic debt of forest biodiversity, changes in forest stand characteristics may modulate the climatic debt by locally modifying microclimatic conditions. Notably, the buffering effect of the upper canopy layer implies microclimate dynamics that may provide more time for understory plant communities to locally adapt.

Keywords

Biodiversity, climate change, climatic debt, anthropogenic disturbances, long-term monitoring, plant community, thermophilization

Introduction

Climate change induces a global redistribution of biodiversity at various spatial scales, with profound consequences on ecosystem functioning and the provision of ecosystem services (Hooper *et al.*, 2012; Pecl *et al.*, 2017). Typical biodiversity redistribution consists of species shifting their geographical range poleward in latitude and/or upslope in elevation (Lenoir & Svenning, 2015), tracking shifting isotherms through colonization and local extinction processes (Jump & Peñuelas, 2005; Dullinger *et al.*, 2012). Locally, changes in species' abundance and population dynamics, preceding species range shifts, are leading to important re-assemblages in community composition (Hillebrand *et al.*, 2010; Walther, 2010). For example, some studies reported that local species assemblages are increasingly dominated by warm-adapted species (i.e. species from lower elevations and/or latitudes) at the expense of cold-adapted species (i.e. species from higher elevations and/or latitudes), a process referred to as "thermophilization" of communities (Gottfried *et al.*, 2012; De Frenne *et al.*, 2013; Zellweger *et al.*, 2020). However, species and communities may respond asynchronously and most likely with time lags relative to the forcing environmental changes, so that plant species assemblages shifting from one equilibrium state to another may not reflect environmental conditions prevailing at the time of the survey but may rather reflect former environmental conditions (Davis, 1984, 1989; Blonder *et al.*, 2017). Such discrepancies between the observed velocity of climate change and the slower velocities at which species and communities are actually responding have been termed "climatic debt" (i.e. the fact

that biotic responses are lagging behind climate change) (Menéndez *et al.*, 2006; Bertrand *et al.*, 2011, 2016; Devictor *et al.*, 2012; Zellweger *et al.*, 2020).

To assess the magnitude of the climatic debt or lag between the velocity of mean annual temperature (MAT) changes and the velocity of thermophilization of communities, one needs first to quantify the degree of thermophilization of local species assemblages. The most straightforward approach is to compute the community temperature index (CTI) (Devictor *et al.*, 2008; Zellweger *et al.*, 2020). The CTI is the average value of either individual species' thermal optima or species-indicator values for temperature across all species co-occurring in a focal community. How CTI changes over time (i.e. the proportion of cold- and warm-adapted species appearing or disappearing from the focal community) likely reflects how communities are responding to climate changes (Devictor *et al.*, 2008; Bertrand *et al.*, 2011). This index thus provides an intuitive proxy to estimate the velocity of thermophilization of communities, and can be subsequently compared to the velocity of observed temperature changes (e.g. both expressed in units of degrees Celsius per decade; Devictor *et al.*, 2008). Changes in CTI (or analogous index) over time have already been used to document thermophilization and delayed biotic responses of a wide range of taxonomic groups (e.g. plants, butterflies, fishes and birds; Devictor *et al.*, 2012; Bertrand *et al.*, 2011; Cheung *et al.*, 2013; Gaüzère *et al.*, 2017). However, most of these studies relied on a relatively restricted number of observations over time, usually a baseline survey and one or two resurveys at best, to compute changes in CTI values over time (Savage & Vellend, 2015; Ash *et al.*, 2017; Fadrique

et al., 2018). Some previous studies even relied on non-permanent or quasi-permanent plots to assess changes in CTI values over time (Bertrand *et al.*, 2011; De Frenne *et al.*, 2013; Becker-Scarpitta *et al.*, 2019; Zellweger *et al.*, 2020). Unfortunately, such studies relying on non-permanent plots tend to infer temporal changes blurred by space-for-time substitutions, which are known to overestimate the magnitude of thermophilization of communities in response to contemporary climate warming (Elmendorf *et al.*, 2015). Even when studies rely on strictly permanent plots, it requires more than one or two resurveys to build a detailed time series of community composition changes from long-term monitoring programs. Strictly permanent monitoring programs relying on frequent resurveys (e.g. from one-year to five-year intervals) during a sufficiently long time period (e.g. at least two decades) are needed to capture a temporal dynamic in the velocity of community thermophilization and confirm linearity over time. Although such long-term time series of biodiversity monitoring already exist (Dornelas *et al.*, 2018), we still lack a good knowledge and understanding of the temporal dynamic of the climatic debt.

Whether the climatic debt of plant communities is steadily growing over time and what are the main underlying determinants of this dynamic remain open questions in global change ecology (Essl *et al.*, 2015; Bertrand *et al.*, 2016; Zellweger *et al.*, 2020). For instance, a previous study focusing on temperate forests has suggested an increasing climatic debt in the response of understory plant communities from the lowlands (Bertrand *et al.*, 2011). A follow-up study has revealed that this growing climatic debt involved a complex combination of abiotic

and biotic factors with the greatest effect size captured by environmental conditions during the baseline surveys (i.e. a greater climatic debt for plant communities occurring within initially warmer conditions) (Bertrand *et al.*, 2016). Noteworthy, the same authors also found that anthropogenic disturbances contributed very little and unexpectedly to the climatic debt. Yet, previous and more recent findings suggest the opposite with local disturbances amplifying forest community responses to climate change (De Frenne *et al.*, 2013; Stevens *et al.*, 2015; Perring *et al.*, 2018; Brice *et al.*, 2019). A more recent study has even demonstrated that the climatic lag in forest plant communities is primarily controlled by forest microclimate dynamics suggesting forest stand characteristics to be a strong determinant of the climatic debt (Zellweger *et al.*, 2020). These discrepancies call for more in-depth investigations on the temporal dynamic of the climatic debt in forest understory plant communities and the relative contribution of anthropogenic and natural disturbances.

In addition to baseline environmental conditions and stand characteristics modulated by anthropogenic and natural disturbances, ungulates directly impact vegetation dynamics (Post & Pedersen, 2008; Olofsson *et al.*, 2009; Boulanger *et al.*, 2018). On the one hand, Olofsson *et al.* (2009) have shown that herbivores inhibit the climate-driven shrub expansion towards high latitudes, indicating that herbivores could contribute to the climatic debt. On the other hand, Post & Pedersen (2008) have shown that plant community composition (e.g. dwarf birch, willow, graminoids, forbs and mosses) on warmed plots (open-top chambers) did not differ

from that on ambient plots where herbivores grazed, suggesting no effect of herbivory on the climatic debt. Altogether, these findings show contrasting impacts of herbivory on the climatic debt.

Here, we rely on a long-term (1995-2017) national (France) monitoring network of permanent forest plots organized in a paired design of exclosure (fenced area excluding ungulates) *vs.* control plots – the RENECOFOR monitoring program – with multiple resurveys (every year to every five years) to generate a high-resolution and unprecedented time series of CTI values for understory plant communities inside and outside the fenced area. Using this information-rich time series, we aimed to: (i) compare the rates of CTI changes to the velocity of MAT changes during the period 1995-2017; (ii) test whether the climatic debt of understory plant communities increased steadily over time; and (iii) assess the relative contribution of several abiotic and biotic factors known to be influential from the scientific literature, including baseline environmental conditions, stand characteristics that are influenced by anthropogenic and natural disturbances, and biotic disturbances from large herbivores.

Materials and Methods

A long-term national monitoring network of forest ecosystems

To assess changes in understory plant communities, we used vegetation data collected every five years, and even every year for some sites, throughout a long-term French monitoring network of forest ecosystems (RENECOFOR,

http://www1.onf.fr/renecofor). The RENECOFOR network belongs to the European ICP Forests Level II monitoring program (ICP Forests, http://www.icp-forests.org) and aims at monitoring the health and functioning of forest ecosystems. This monitoring network was established in 1992 by the French National Forest Service (ONF, Office National des Forêts). It includes 102 permanents plots distributed in state and communal forests throughout the whole metropolitan French territory (www1.onf.fr/renecofor/sommaire/sites) (Ulrich, 1995 ; Nicolas *et al.*, 2014). All plots are located in mature and even-aged pure stands, and cover an area of 2 ha with a central fenced zone of 0.5 ha to exclude large herbivores (**Fig. 1**) (for more details, see Boulanger *et al.*, 2018).

Since 1995, vegetation surveys have been conducted every five years (baseline survey in 1995 and resurveys in 2000, 2005, 2010 and 2015). From the total pool of 102 permanent plots, we discarded 58 plots which suffered from major data gaps throughout the studied time period (e.g. the resurvey of 2010 was systematically missing for 53 plots due to a shortage in funding). This yielded a total of 44 plots for which a full time series, at a 5-yr interval, was available between 1995 and 2015, hereafter referred to as the five-year dataset (**Fig. 1**). Among these 44 plots, 8 plots were monitored annually without discontinuity between 1995 and 2017, hereafter referred to as the yearly dataset (**Fig. 1**). The whole workflow of analyses was carried out separately for both the five-year and yearly datasets, as these two datasets are very complementary (*Supporting Information App. Fig. 1*). Although the five-year dataset covers a large spatial extent representative of all temperate

forests in France, its temporal resolution is rather coarse. *Per contra*, the yearly dataset covers a restricted spatial extent but provides a very detailed time series at high temporal resolution. More information on the spatial location and dominant tree species for each of 44 study plots are provided in *Supporting Information App. Table 1*.

During each monitoring campaign, the vegetation was surveyed by expert botanists according to standardized protocols under a quality assurance and quality control procedure. The quality assurance and quality control procedure involved intercalibration exercises organized the year before each monitoring campaign with all expert botanists surveying the same plots in the same forest (Camaret & Brêthes, 2004; Archaux *et al.*, 2009). During each monitoring campaign, all plots were surveyed both at spring and in summer/autumn, to cover the entire growing season. All vascular plants were recorded in eight 2 m × 50 m subplots: four inside and four outside the fenced area of 0.5 ha (**Fig. 1**). The cover-abundance of all taxa occurring in four vegetation layers (tree: > 7 m; high shrub: 2–7 m; low shrub: 0.3–2 m; herb: < 0.3 m) was recorded. Species names were standardized following the nomenclature of *Flora Europaea* (Tutin *et al.*, 2001). A total of 877 taxa were recorded in all vegetation layers, including 751 occurring in the herb layer (hereafter understory plants). Here, we restricted our analyses to understory plants, including tree seedlings, because they represent a relevant component of forest biodiversity which is not directly (but indirectly via the upper canopy layers) impacted by forest management practices, and are expected to be the most

responsive to climate warming. Only taxa identified at the species or subspecies levels were kept for analyses. Identifications at the genus level were considered as incomplete and excluded from our analyses (i.e. 80 taxa excluded; see the list of species provided in *Supporting Information App. Table 2*). Our dataset encompassed a total of 782 vegetation records, including 347 records from the yearly dataset (492 species) and 435 records from the five-year dataset (593 species). Seasonal surveys (spring and summer/autumn) were aggregated by year with the maximum cover-abundance coefficient retained whenever a species was recorded at both dates. This yielded to a total of 186 and 220 vegetation records for the yearly and five-year dataset, respectively.

Time series of temperature data

To compare the velocity of mean annual temperature (MAT) changes with the velocity of temperature changes inferred from understory plant communities, we first extracted time series of MAT changes. We obtained macroclimate temperature time series from the global dataset TerraClimate (Abatzoglou *et al.*, 2018), which provides monthly climate data for every year from 1958 up to 2018 at a spatial resolution of 2.5 arc-minute (~3.3 km × 4.64 km at 45° of latitude). We also extracted climatic time series from the CHELSA database (Karger *et al.*, 2017) but found very similar trends between TerraClimate and CHELSA (*Supporting Information App. Fig. 2*). Thus, we decided to use only TerraClimate in our subsequent analyses as it better covers the end of our study period (i.e. 2017). As TerraClimate provides only maximum and minimum monthly temperatures, we first calculated the monthly

mean for each of the 44 studied plots (by averaging maximum and minimum temperature values for each month), and then computed mean annual temperature (hereafter MAT) for each year between 1958 and 2017. Between 1958 and 2017, MAT increased across all 44 studied plots, leading to a shift from negative to only positive anomalies towards the end of the reference period (1958–2017) (*Supporting Information App. Fig. 3*). From the very beginning (1992) of the RENECOFOR monitoring program until 2017, anomalies were mostly positive (values ranging from -0.56 to 1.54 over the period 1992-2017), except for three years (1993, 1996 and 2010), for which anomalies were negative.

To infer temperature conditions from local species assemblages, we used the community temperature index (CTI) (Devictor *et al.*, 2008, 2012) (see Equation 1). The CTI was computed based on occurrence data by averaging the indicator values (IVs) for temperature across all species i (Sp_i) occurring in a given relevé j (containing S species, with $S \geq 2$). Here, we used presence/absence data instead of weighting IVs by each species' abundance/dominance in the relevés. We did that to give the same weight to common and rare species. As each RENECOFOR plot includes 8 subplots, we calculated the CTI values at the subplot level and kept this information at the subplot level without aggregating it at the plot level.

(1) $$CTI_j = \frac{\sum_{i=1}^{S} IV\ Temperature\ Sp_i}{S}$$

Species' IVs for temperature were extracted from both the CATMINAT (Julve, 1998) and EcoPlant (Gégout *et al.*, 2005) databases, and we used them in combination to take advantage of their respective strengths (*Supporting Information App. Fig. 4*).

On the one hand, the CATMINAT database is based on expert knowledge similarly to Ellenberg's IVs (Ellenberg et al., 1992), with temperature preferences of plant species coded along an ordinal scale from cold (1) to warm (9) conditions. It contains almost all of species recorded in our dataset (858 out of the 877 species recorded in all vegetation layers), but CTI values are unitless and direct comparisons with macroclimatic temperatures are not possible. On the other hand, EcoPlant IVs for temperature are directly expressed in degrees Celsius (Gégout et al., 2005) allowing the direct computation of CTI values in degrees Celsius, but much less species from our dataset are recorded (396 out of 877 species). Based on these two databases, we calibrated a transfer function to produce CTI values directly expressed in degrees Celsius and transform the unitless CTI values from the CATMINAT database into a CTI value expressed in degrees Celsius (*Supporting Information App. Fig. 4 & 5*; and see Lenoir *et al.*, 2013 for a similar approach).

Based on the time series of MAT values and the time series of CTI values, both expressed in degrees Celsius, we computed the lag as the difference between the two (MAT − CTI), thus getting a new time series of the difference: the climatic debt (Bertrand *et al.*, 2016).

The main determinants of the climatic debt

Although we were primarily interested in assessing the temporal dynamic of the difference between MAT and CTI values, thereby testing the effect of time itself on the direction and magnitude of this difference – as we assumed the climatic debt to

increase over time – we also assessed the relative contributions of several abiotic and biotic determinants known to potentially modulate the climatic debt. For instance, it has already been demonstrated that MAT during or prior to the baseline survey was a strong and positive determinant of the climatic debt in understory plant communities, suggesting greater lags in initially warmer areas (Bertrand *et al.*, 2016). Hence, to account for that potential confounding effect, we computed baseline temperature conditions from TerraClimate as the average of MAT values during the 1961-1990 reference period (i.e. 30-yr average typically used to capture long-term climatic conditions) and added it as a covariate to explain the climatic debt.

In addition to baseline temperature conditions, we gathered information on anthropogenic and natural disturbances, and stand characteristics, all available from the RENECOFOR monitoring program. Because local disturbances may have significant effects on understory plant communities and are known to accelerate their thermophilization rates and reduce the climatic debt (Bengtsson *et al.*, 2000; Stevens *et al.*, 2015; Brice *et al.*, 2019), we built several variables capturing these local disturbances (*Supporting Information App. Fig. 6 & 7*). First, we distinguished between natural (e.g. windstorm) and anthropogenic disturbances (i.e. local disturbances associated to forest management practices such as thinning, cleaning and tree extraction). For each of these two types of disturbances, we computed the cumulative sum of disturbance events occurring within a given forest plot prior to each survey year. Here, we assumed that repeated disturbance events are likely to

accelerate the thermophilization rate and thus reduce the climatic debt of understory plant communities. Then, irrespective of the type of disturbance, we also computed the anteriority, i.e. the number of years, between the last disturbance event and the year of the survey, assuming that a very short anteriority (less than a year) will impact less the difference between MAT and CTI values. Indeed, plant community composition is unlikely to change during the vegetation season that is just following a stand thinning event. However, significant changes in plant community composition may lag and happen during the next couple of years with light demanding and warm-adapted species germinating from the soil seed bank and increasing CTI values, thus paying off part of the climatic debt. We also retrieved information about stand characteristics at the plot level, including: stand basal area during the monitoring year; stand age in 1995; and the type of dominant tree species (i.e. deciduous *vs.* coniferous). We hypothesized that plots with higher stand basal area and located in older forest stands are likely to be more buffered against the adverse effect of macroclimate warming (Zellweger *et al.*, 2019), thus further inflating the climatic debt of understory plant communities (De Frenne *et al.*, 2013). The exclosure effect (i.e. fenced area excluding ungulates and large herbivores vs. control plots outside the fenced area) was added as a covariate in all our analyses on the temporal trends in CTI values and the climatic debt. According to the scientific literature, climate change impacts on vegetation dynamics tend to be inhibited by large herbivores (Post & Pedersen, 2008; Kaarlejärvi *et al.*, 2013), hence we hypothesized a greater climatic debt outside than inside the fenced area.

Statistical analyses

We used linear mixed-effects models (LMMs) to assess the velocity of MAT changes and thermophilization of understory plant communities. For CTI values, we used the continuous variable "year" of the monitoring as the main fixed effect while accounting for potentially diverging temporal dynamics between the outside and inside of the fenced area, by adding the interaction effect: year × exclosure. The RENECOFOR plot ID (44 or 8 levels depending on the dataset used) and the vegetation subplot ID (8 levels), nested within the plot ID, were used as a random term to account for the hierarchical structure of the sampling design and the repeated surveys over time. For MAT values, we only used the "year" of the monitoring as a fixed effect and the RENECOFOR plot ID as a random term. Indeed, for MAT, the subplot level was not used in the random component of LMMs since all 8 subplots within a given plot have similar MAT values. To allow between-site variation in the temporal dynamics of MAT and CTI values, we set the random term (e.g. plot ID) of our LMMs so that it modifies the slope coefficient (i.e. random slope term) of the variable "year" for each level of the random term variable. The coefficient estimate of the "year" variable in our LMMs was used as a proxy for estimating the velocities of temperature changes, both for MAT and CTI values. Assumptions of normality and homoscedasticity of the residuals of our models were visually checked and no departure from normality and homoscedasticity were detected. Significance of the predictors in LMMs were assessed using Wald χ^2 tests, after fitting models with the restricted maximum likelihood estimation.

To analyze the temporal dynamic of the difference between MAT and CTI values over time (i.e. the climatic debt), we used LMMs with the value of the difference (MAT − CTI) as the response variable and the continuous variable "year" of monitoring as the main fixed effect variable. In addition to "year", we added several abiotic and biotic covariates as fixed effect variables to assess their relative contribution in modulating the climatic debt. These covariates were: baseline temperature conditions; sum of natural disturbances; sum of anthropogenic disturbances; disturbance anteriority; stand basal area; stand age; type of dominant tree species in forest stand (deciduous *vs.* coniferous); and the exclosure effect. From the full model including all covariates together with time as fixed effect terms, we ran all possible combinations of models and ranked all candidate models using the corrected Akaike information criteria (AICc). Based on the best candidate model with the lowest AICc value, we then computed the difference in AICc values (ΔAICc) for all models relative to the best candidate model. Finally, from the set of selected candidate models with ΔAICc values < 2, we used a model averaging approach to calculate the conditional mean value of each coefficient and its associated 95% confidence interval (Burnham & Anderson, 2002). All continuous predictor variables were standardized (*z*-score) before analyses to improve their interpretability on a comparable scale (Schielzeth, 2010). None of the fixed-effect variables included in our models showed multicollinearity issues (VIF < 3; Zuur *et al.*, 2007). Note that correlation values among all our explanatory variables did not exceed a Spearman's r coefficient of 0.6 (*Supporting Information App. Fig. 8*). Again, we used the RENECOFOR plot ID (44 or 8 levels depending on the dataset used) and the

vegetation subplot ID (8 levels), nested within the plot ID, as a random slope term modifying the effect of "year" of monitoring. The explained variance of LMMs was determined by calculating the marginal (R^2m, associated with fixed effects only) and conditional (R^2c, associated with both fixed and random effects) R^2 values (Nakagawa & Schielzeth, 2013) using the `r.squared.GLMM` function from the `MuMIn` package.

All statistical analyses were performed with the R software version 3.6.0 (R Core Team, 2019). Models were performed with the `nlme` package v.3.1-140 (Pinheiro *et al.*, 2019), and the model selection procedure was assessed with the `MuMIn` package v.1.43.6 (Bartoń, 2019), using the `dredge` function. Other packages were used for data handling extraction and graphical visualization: `dplyr` v.0.8.3 (Wickham *et al.*, 2019); `raster` v.2.9-23 (Hijmans, 2019); `ggplot2` v.3.2.0 (Wickham, 2016); `cowplot` v.1.0.0 (Wilke, 2019); and `sf` v.0.7-7 (Pebesma, 2018).

Results

Temporal trends in macroclimate and community temperatures

Using the 5-yr interval dataset, mean annual temperature (MAT) during 1995–2015 increased by 0.23 ± 0.02 °C/decade (95 % Confidence Intervals (CI): 0.18-0.28, t = 9.05, P < 0.001; **Fig. 2a**). In the yearly dataset, MAT increased by 0.31 ± 0.05 °C/decade (95 % CI: 0.20-0.42, t = 5.51, P < 0.001; **Fig. 2b**) during 1995–2017. Over the same time periods, the velocities of CTI changes were weaker, but similar trends and magnitudes were observed in both the five-year (0.10 ± 0.03 °C/decade, 95 %

CI: 0.04-0.15, $t = 3.62$, $P < 0.001$; **Fig. 2a**) and yearly (0.08 ± 0.03 °C/decade, 95 % CI: 0.01-0.14, $t = 2.15$, $P = 0.031$; **Fig. 2b**) datasets. No significant differences were observed in CTI trends between inside and outside of the fenced area. Further, the difference between MAT and CTI values showed a tendency to increase steadily over time (**Fig. 2**): the lag in the response of herbaceous plant communities to climate warming increased linearly over time. Although we found a significant effect of time, it contributed weakly to the overall variation in MAT and CTI values: $R^2m \leq 0.01$ while R^2c ranged between 0.92 to 0.96.

Factors contributing to the climatic debt

For both the yearly and five-year datasets, the model averaging procedure to explain the climatic debt (MAT − CTI) selected 4 and 3 candidate models (ΔAICc < 2), respectively. The best candidate models explained 55% and 70% of the total variation in the difference between MAT and CTI values for the five-year (R^2m = 0.33; R^2c = 0.55) and yearly (R^2m = 0.46; R^2c = 0.70) datasets, respectively. The best candidate model for the five-year dataset contained 6 variables including the year of sampling, stand age, the anteriority of the last disturbance, the cumulative number of anthropogenic disturbances, stand basal area, and baseline temperature conditions. For the yearly dataset, the best candidate model included the same 6 variables together with the type of dominant tree species (*Supporting Information App. Tables 3 & 4 and App. Fig. 9 & 10*).

Irrespective of the dataset considered in our analyses, we found very consistent and similar trends in the factors contributing to the climatic debt (**Fig. 3**). For instance, the year of sampling had a positive effect on the magnitude of the difference, confirming an increasing climatic debt of understory plant communities over time (five-year dataset = 0.06 ± 0.03 SE, *Fig. 3a*; yearly dataset = 0.31 ± 0.04 SE, *Fig. 3b* and *Fig. 4a*).

Baseline temperature conditions had the strongest positive influence on the climatic debt (five-year dataset = 0.77 ± 0.04 SE, *Fig. 3a*; yearly dataset = 0.72 ± 0.10 SE, *Fig. 3b*), indicating greater lags in plots with warmer baseline temperature conditions during the period 1961–1990. We also found a positive effect of stand characteristics, through the variables stand age in 1995 and basal area during the year of monitoring, on the magnitude of the lag. More specifically, the lag was larger in denser (five-year dataset = 0.22 ± 0.04 SE, *Fig. 3a*; yearly dataset = 0.35 ± 0.05 SE, *Fig. 3b* and *Fig. 4b*) and older (five-year dataset = 0.15 ± 0.04 SE, *Fig. 3a*; yearly dataset = 0.46 ± 0.07 SE, *Fig. 3b* and *Fig. 4c*) forests. We found no clear differences in the climatic debt between coniferous and deciduous forests as well as between inside and outside of the fenced area.

In contrast, forest disturbance had a negative effect on the climatic debt (*Fig. 3*). Notably, the magnitude of the lag was negatively correlated with the anteriority of the last disturbance event (five-year dataset = -0.12 ± 0.02 SE, *Fig. 3a*; yearly dataset = -0.10 ± 0.03 SE, *Fig. 3b*), revealing that lags decrease in plots recently disturbed. Moreover, the cumulative number of anthropogenic disturbances were

negatively correlated to the climatic debt (five-year dataset = -0.17 ± 0.04 SE, *Fig. 3a*; yearly dataset = -0.19 ± 0.07 SE, *Fig. 3b*), indicating that lags decrease in the most frequently disturbed plots, following logging events. The cumulative number of natural disturbances was only retained in the models based on the five-year dataset, albeit its tendency towards a negative effect did not differ from zero (-0.04 ± 0.04 SE, *Fig. 3a*).

Discussion

Velocities of thermophilization

Irrespective of the temporal resolution in the data (i.e. the yearly vs. five-year dataset), we show a very similar increase in temperature conditions inferred from understory plant communities over the period 1995–2017, consistent with a thermophilization process. This finding adds to a growing body of evidence describing thermophilization of plant communities across many forest ecosystems around the globe (e.g. in temperate, boreal and tropical ecosystems; Lenoir *et al.*, 2010; Bertrand *et al.*, 2011; De Frenne *et al.*, 2013; Savage & Vellend, 2015; Fadrique *et al.*, 2018; Zellweger *et al.*, 2020), as well as across other ecosystems and taxonomic groups (e.g. in mountain plant communities, Gottfried *et al.*, 2012; marine fishes and invertebrates, Cheung *et al.*, 2013; birds and butterflies, Devictor *et al.*, 2012; bumblebee communities, Fourcade *et al.*, 2018). The velocities of thermophilization we report here (ranging from 0.08 to 0.10 °C/decade) are broadly in the range of those reported in the scientific literature (from 0.03 to 0.38

°C/decade; *Supporting Information App. Table. 5*), but also are among the highest rates recorded for plant communities (maximum value of 0.27 °C/decade; Duque *et al.*, 2015). Specifically, we show velocities that are twice as fast as the average thermophilization rate estimated for understory plant communities across temperate deciduous forests in Europe (i.e. 0.041 °C/decade; De Frenne *et al.*, 2013). Nevertheless, these rates are still much lower than those found in marine ecosystems, where environmental constraints may weakly limit the dispersal of species in response to rising temperatures (Lenoir *et al.*, 2020).

Our findings consist in the most recent updates supporting and consolidating previous reports of plant community thermophilization which happened across the same study area (France) (Bertrand *et al.*, 2011; Martin *et al.*, 2019). Focusing on a completely independent dataset from the period 1965–2008, Bertrand *et al.* (2011) were the first to highlight a thermophilization of understory plant communities in the French forests. More recently, Martin *et al.* (2019) have described a similar thermophilization trend extending to other plant communities at national and regional scales in France over the period 2009–2017. Unlike these previous studies relying either on massive collection of opportunistic surveys over time (Bertrand *et al.*, 2011) or citizen science data (Martin *et al.*, 2019), our study is the first that used a long-term monitoring program based on strictly permanent plots intensively monitored over time (up to every year), providing a very detailed time series of changes in understory plant community composition. Hence, we argue that the velocities we report here do not suffer from biases due to space-for-time

substitutions and are thus likely to be more accurate than those previously reported (Elmendorf *et al.*, 2015), which matters for informing our society on future scenarios of biodiversity changes (IPBES, 2019). Furthermore, our yearly resurveys over a period of 25 years confirm that the thermophilization rate of understory plant communities in temperate forests is following a linear trajectory over time. This is an important and novel finding that helps us to understand the temporal dynamic of the biotic responses to anthropogenic climate change. Yet, time alone had a very minor contribution to explain the variation in temperature conditions inferred from understory plant communities. This suggests that other abiotic and biotic determinants, such as the macroclimatic context as well as local stand characteristics influenced by anthropogenic disturbances may potentially explain local variations in temperature conditions.

The climatic debt and its potential determinants

One of our most striking results is that the velocity at which atmospheric air temperatures are rising is twice faster, on average, than the velocity at which understory plant communities are responding, generating a climatic debt that is steadily growing over time, even after accounting for the relative contribution of several abiotic and biotic determinants modulating it. Although the idea of an increasing climatic debt over time has already been suggested (Bertrand *et al.*, 2011), we provide the first evidence that the climatic debt of understory plant communities in response to the ongoing climate change is steadily increasing over time. This contrasts with a previous report showing no clear temporal signal in the

climatic debt of herbaceous plant communities in French forests (Bertrand *et al.*, 2016). Considering the velocity of the predicted future climate change (Loarie *et al.*, 2009), this is an important result because it raises the question whether the lag will continue to steadily accumulate and approach a potential critical breakpoint for understory biodiversity and forest ecosystem functioning. Interestingly, the linear increase of the climatic debt over time is clearer and more pronounced (higher effect size) in the yearly dataset than in the five-year dataset. This is probably because the long-term increasing trend in the climatic debt was better separated from inter-annual variations in the yearly dataset than in the five-year dataset. Inter-annual variations tend to play a bigger role in blurring the long-term response of understory plant communities when the frequency between resurveys is lower.

Importantly, we demonstrate that forest stand characteristics and anthropogenic disturbances significantly matter in modulating the climatic debt, by either increasing (positive effect) or mitigating (negative effect) the lag. For instance, both the anteriority of the last disturbance event and the cumulative number of anthropogenic disturbances have a negative effect on the climatic debt. Such findings are in accordance with recent works indicating that local disturbances speed up the process of thermophilization in plant communities (Stevens *et al.*, 2015; Brice *et al.*, 2019; Zellweger *et al.*, 2020). However, it remains to be investigated in more details whether the thermophilization of understory plant communities following anthropogenic disturbances is due to warm-adapted species that are: (i) replacing more mesophilous species (pure turnover); (ii) increasing the

local species pool (nestedness); or both simultaneously. For instance, Closset-Kopp *et al.* (2018) have shown that understory plant communities in heavily managed forest stands had the tendency to be richer in warm-adapted species in 2015 than in 1970, mostly due to an increase in local species richness but no species turnover. In our study, both processes seem to occur. Indeed, while the total number of species per plot increases over time, suggesting a process of nestedness, the set of warm-adapted species that are colonizing (i.e. species gain) the plots of our monitoring network between 1995 and 2015 are also replacing relatively more mesic species that are disappearing (i.e. species loss) (*Supporting Information, App. Fig. 11*), suggesting a process of turnover. Not only the richness of warm-adapted species increases at the expense of cold-adapted species, but this effect is concomitant with a relative increase in the richness of light- and nitrogen-demanding species at the expense of species tolerating shade conditions and nitrogen-poor soils (*Supporting Information, App. Fig. 12*). These trends further confirm the importance of local disturbances as key factors modulating the lag between macroclimatic conditions and plant community thermophilization. Noteworthy, our results contrast with those from Bertrand *et al.* (2016), who reported non-significant effects of anthropogenic disturbances on the climatic debt of understory plant communities. Looking at the effects of stand characteristics, our results underline the key role of stand age and basal area to modulate the climatic debt. Older and denser (high basal area) forest stands provide particular microclimatic conditions (e.g. cooler ground-level temperatures due to increased shading and humidity conditions) that are likely to buffer the adverse effects of macroclimatic warming on understory

plant communities thus providing thermal microrefugia for species persistence (Lenoir *et al.*, 2017; De Frenne *et al.*, 2019; Zellweger *et al.*, 2020). In contrast, repeated disturbances are likely to create canopy openings in forest stands, modifying the microhabitat and associated microclimate that strongly exacerbate the impact of macroclimate temperature warming for understory vegetation (Vanderwel & Purves, 2014; Zellweger *et al.*, 2020). This can in turn lead to drastic changes in the overall composition of the plant community (i.e. by increasing the proportion of warm-adapted species through either species turnover or an increase in local species richness) that will reduce the climatic debt. Paying off the climatic debt of understory plant communities in temperate forests implies to break off this microclimate stability, which can consequently reduce the microrefugia capacity of forest habitats for the survival of forest-dwelling species under anthropogenic climate change (Lenoir *et al.*, 2017). Accepting the idea that the climatic debt of understory plant communities might be a positive sign of local adaptation has significant implications on the concept of climatic debt itself, which might be interpreted as a macroclimatic debt but not a microclimatic debt.

Contrary to our initial expectation that large herbivores should contribute to the climatic debt by further increasing the lag in the response of understory plant communities to macroclimate warming, we found no difference in the observed climatic debt between outside and inside the fenced area. This suggests that the climatic debt generated by the buffering effect of microclimate in the understory may mostly stem from the canopy layer and independently from the shrub layer, as

large herbivores are mostly impacting woody species from the understory shrub layer (Olofsson *et al.*, 2009; Boulanger *et al.*, 2018). The indirect effects of herbivores on vegetation responses to climate warming can be highly dependent on the ecological context, as pointed out by Vuorinen *et al.*, (2020).

Together with previous studies, our results show that the climatic debt in understory plant communities seem to be much more pronounced in situations where temperature conditions were warmer during the period preceding the baseline surveys (Bertrand *et al.*, 2016), such as in the lowlands (Bertrand *et al.*, 2011). However, the fact that warmer baseline conditions increase the climatic debt of understory plant communities could also stem from a bias towards an underestimation of CTI values in communities where immigrating species can only come from even warmer regions likely outside the calibration range used to compute the CTI values. This could therefore lead to a systematic overestimation of the observed climatic debt in the warmest part of the study area. This hypothesis is supported by the extreme values observed in the distribution of indicator values (IVs) from the EcoPlant database (*Supporting Information App. Fig. 5*), which may indicate that the model calibration range is too limited and should be extended to other environmental conditions (i.e. here, the Mediterranean regions to capture the pool of immigrating species coming from for warmer conditions). This potential bias supports general recommendations to take into account existing differences in sensitivity between species pools when assessing temporal changes in CTI values (Burrows *et al.*, 2019; Williams *et al.*, 2020). More data on species IVs, either expert-

based or biogeographically-derived IVs, are needed from warmer regions to improve estimates of CTI values in the current context of global warming.

Conclusion

This study shows that the thermophilization of understory plant communities in French forests continued during the last two decades with rapid but insufficient rates to track the velocity of current climate warming, leading to a steadily increase in the climatic debt. Additionally, we report that forest stand structure and anthropogenic disturbances can be modulated to increase or decrease the climatic debt. For instance, the positive effect of denser and older canopy layers on forest microclimate dynamics could inflate the climatic debt of understory plant communities and provide more time for understory plant communities to locally adapt. However, it remains uncertain how big the climatic debt can grow over time before a tipping point is reached such that the climatic debt will suddenly be paid off. For instance, repeated drought events leading to extensive tree dieback and massive crown defoliation could exceed this tipping point by suddenly recoupling the understory layer with macroclimatic conditions prevailing outside forests. Such a quick recovery of the climatic debt will have drastic consequences on forest biodiversity and ecosystem functioning.

References

Abatzoglou, J.T., Dobrowski, S.Z., Parks, S.A. & Hegewisch, K.C. (2018) TerraClimate, a high-resolution global dataset of monthly climate and climatic water balance from 1958–2015. *Scientific Data*, **5**, 170191.

Archaux, F., Camaret, S., Dupouey, J.L., Ulrich, E., Corcket, E., Bourjot, L., … Touffet, J. (2009) Can we reliably estimate species richness with large plots? an assessment through calibration training. *Plant Ecology*, **203**, 303–315.

Ash, J.D., Givnish, T.J. & Waller, D.M. (2017) Tracking lags in historical plant species' shifts in relation to regional climate change. *Global Change Biology*, **23**, 1305–1315.

Bartoń, K. (2019) MuMIn: Multi-Model Inference.

Becker-Scarpitta, A., Vissault, S. & Vellend, M. (2019) Four decades of plant community change along a continental gradient of warming. *Global Change Biology*, **25**, 1629–1641.

Bengtsson, J., Nilsson, S.G., Franc, A. & Menozzi, P. (2000) Biodiversity, disturbances, ecosystem function and management of European forests. *Forest Ecology and Management*, **132**, 39–50.

Bertrand, R., Lenoir, J., Piedallu, C., Dillon, G.R., De Ruffray, P., Vidal, C., … Gégout, J.C. (2011) Changes in plant community composition lag behind climate warming in lowland forests. *Nature*, **479**, 517–520.

Bertrand, R., Riofrío-Dillon, G., Lenoir, J., Drapier, J., De Ruffray, P., Gégout, J.C. & Loreau, M. (2016) Ecological constraints increase the climatic debt in forests. *Nature Communications*, **7**.

Blonder, B., Moulton, D.E., Blois, J., Enquist, B.J., Graae, B.J., Macias-Fauria, M., … Svenning, J.-C. (2017) Predictability in community dynamics. *Ecology Letters*, **20**, 293–306.

Boulanger, V., Dupouey, J., Archaux, F., Badeau, V., Baltzinger, C., Chevalier, R., … Ulrich, E. (2018) Ungulates increase forest plant species richness to the benefit of non-forest specialists. *Global Change Biology*, **24**, e485–e495.

Brice, M., Cazelles, K., Legendre, P. & Fortin, M. (2019) Disturbances amplify tree community responses to climate change in the temperate–boreal ecotone. *Global Ecology and Biogeography*, geb.12971.

Burnham, K.P. & Anderson, D.R. eds. (2002) *Model Selection and Multimodel Inference: A Practical Information-Theoretic Approach*. pp. 49–97. Springer-Verlag New York.

Burrows, M.T., Bates, A.E., Costello, M.J., Edwards, M., Edgar, G.J., Fox, C.J., Halpern, B.S., Hiddink, J.G., Pinsky, M.L., Batt, R.D., García Molinos, J., Payne, B.L., Schoeman, D.S., Stuart-Smith, R.D. & Poloczanska, E.S. (2019) Ocean community warming responses explained by thermal affinities and temperature gradients. *Nature Climate Change*, **9**, 959–963.

Camaret, S. & Brêthes, A. (2004) *Suivi de la composition floristique des placettes du réseau (1994/95-2000) et élaboration d'un programme d'assurance qualité intensif*, Office National des Forêts-Direction Technique.

Cheung, W.W.L., Watson, R. & Pauly, D. (2013) Signature of ocean warming in global fisheries catch. *Nature*, **497**, 365–368.

Closset-Kopp, D., Hattab, T. & Decocq, G. (2018) Do drivers of forestry vehicles also drive herb layer changes (1970-2015) in a temperate forest with contrasting habitat and management conditions? *Journal of Ecology*.

Davis, M.B. (1984) *Climatic Instability, Time, Lags, and Community Disequilibrium. Community ecology* Community ecology. (ed. by J.M. Diamond) and T.J. Case), pp. 269–284. Harper; Row.

Davis, M.B. (1989) Lags in vegetation response to greenhouse warming. *Climatic Change*, **15**, 75–82.

De Frenne, P., Rodríguez-Sánchez, F., Coomes, D.A., Baeten, L., Verstraeten, G., Vellend, M., … Verheyen, K. (2013) Microclimate moderates plant responses to macroclimate warming. *Proceedings of the National Academy of Sciences of the United States of America*, **110**, 18561–5.

De Frenne, P., Zellweger, F., Rodríguez-Sánchez, F., Scheffers, B.R., Hylander, K., Luoto, M., … Lenoir, J. (2019) Global buffering of temperatures under forest canopies. *Nature Ecology and Evolution*, **3**, 744–749.

649 Devictor, V., Julliard, R., Couvet, D. & Jiguet, F. (2008) Birds are tracking climate
650 warming, but not fast enough. *Proceedings of the Royal Society B: Biological*
651 *Sciences*, **275**, 2743–2748.

652 Devictor, V., Swaay, C. van, Brereton, T., Brotons, L., Chamberlain, D., Heliölä, J.,
653 … Jiguet, F. (2012) Differences in the climatic debts of birds and butterflies at a
654 continental scale. *Nature Climate Change*, **2**, 121–124.

655 Dornelas, M., Antão, L.H., Moyes, F., Bates, A.E., Magurran, A.E., Adam, D., …
656 Zettler, M.L. (2018) BioTIME: A database of biodiversity time series for the
657 Anthropocene. *Global Ecology and Biogeography*, **27**, 760–786.

658 Dullinger, S., Gattringer, A., Thuiller, W., Moser, D., Zimmermann, N.E., Guisan,
659 A., … Hülber, K. (2012) Extinction debt of high-mountain plants under twenty-first-
660 century climate change. *Nature Climate Change*, **2**, 619–622.

661 Duque, A., Stevenson, P.R. & Feeley, K.J. (2015) Thermophilization of adult and
662 juvenile tree communities in the northern tropical Andes. *Proceedings of the*
663 *National Academy of Sciences of the United States of America*, **112**, 10744–10749.

664 Ellenberg, H., Weber, H.E., Düll, R., Wirth, V., Werner, W. & Paulißen, D. (1992)
665 Zeigerwerte von Pflanzen in Mitteleuropa. *Scripta Geobotanica*.

666 Elmendorf, S.C., Henry, G.H.R., Hollister, R.D., Fosaa, A.M., Gould, W.A.,
667 Hermanutz, L., … Walker, M. (2015) Experiment, monitoring, and gradient methods
668 used to infer climate change effects on plant communities yield consistent patterns.

Proceedings of the National Academy of Sciences of the United States of America, **112**, 448–52.

Essl, F., Dullinger, S., Rabitsch, W., Hulme, P.E., Pyšek, P., Wilson, J.R.U. & Richardson, D.M. (2015) Delayed biodiversity change: no time to waste. *Trends in Ecology & Evolution*, **30**, 375–378.

Fadrique, B., Báez, S., Duque, Á., Malizia, A., Blundo, C., Carilla, J., … Feeley, K.J. (2018) Widespread but heterogeneous responses of Andean forests to climate change. *Nature*.

Fourcade, Y., Åström, S. & Öckinger, E. (2018) Climate and land-cover change alter bumblebee species richness and community composition in subalpine areas. *Biodiversity and Conservation*.

Gaüzère, P., Princé, K. & Devictor, V. (2017) Where do they go? The effects of topography and habitat diversity on reducing climatic debt in birds. *Global Change Biology*, **23**, 2218–2229.

Gégout, J.C., Coudun, C., Bailly, G. & Jabiol, B. (2005) EcoPlant: A forest site database linking floristic data with soil and climate variables. *Journal of Vegetation Science*, **16**, 257–260.

Gottfried, M., Pauli, H., Futschik, A., Akhalkatsi, M., Barančok, P., Benito Alonso, J.L., … Grabherr, G. (2012) Continent-wide response of mountain vegetation to climate change. *Nature Climate Change*, **2**, 111–115.

Hijmans, R.J. (2019) raster: Geographic Data Analysis and Modeling.

Hillebrand, H., Soininen, J. & Snoeijs, P. (2010) Warming leads to higher species turnover in a coastal ecosystem. *Global Change Biology*, **16**, 1181–1193.

Hooper, D.U., Adair, E.C., Cardinale, B.J., Byrnes, J.E.K., Hungate, B.A., Matulich, K.L., … Connor, M.I. (2012) A global synthesis reveals biodiversity loss as a major driver of ecosystem change. *Nature*, **486**, 105–108.

IPBES (2019) Summary for policymakers of the global assessment report on biodiversity and ecosystem services of the Intergovernmental science-policy platform on biodiversity and ecosystem services.

Julve, P. (1998) Baseflor: Index botanique, écologique et chorologique de la flore de France. Version 2009.

Jump, A.S. & Peñuelas, J. (2005) Running to stand still: adaptation and the response of plants to rapid climate change. *Ecology Letters*, **8**, 1010–1020.

Kaarlejärvi, E., Eskelinen, A. & Olofsson, J. (2013) Herbivory prevents positive responses of lowland plants to warmer and more fertile conditions at high altitudes. *Functional Ecology*, **27**, 1244–1253.

Karger, D.N., Conrad, O., Böhner, J., Kawohl, T., Kreft, H., Soria-Auza, R.W., … Kessler, M. (2017) Climatologies at high resolution for the earth's land surface areas. *Scientific Data*, **4**, 170122.

Lenoir, J., Gégout, J.C., Dupouey, J.L., Bert, D. & Svenning, J.C. (2010) Forest plant community changes during 1989-2007 in response to climate warming in the Jura Mountains (France and Switzerland). *Journal of Vegetation Science*, **21**, 949–964.

Lenoir, J., Graae, B.J., Aarrestad, P.A., Alsos, I.G., Armbruster, W.S., Austrheim, G., … Svenning, J.C. (2013) Local temperatures inferred from plant communities suggest strong spatial buffering of climate warming across Northern Europe. *Global Change Biology*, **19**, 1470–1481.

Lenoir, J., Hattab, T. & Pierre, G. (2017) Climatic microrefugia under anthropogenic climate change: implications for species redistribution. *Ecography*, **40**, 253–266.

Lenoir, J. & Svenning, J.-C. (2015) Climate-related range shifts - a global multidimensional synthesis and new research directions. *Ecography*, **38**, 15–28.

Lenoir, J., Bertrand, R., Comte, L. *et al.* (2020) Species better track climate warming in the oceans than on land. *Nature Ecology Evolution* **4**, 1044–1059.

Loarie, S.R., Duffy, P.B., Hamilton, H., Asner, G.P., Field, C.B. & Ackerly, D.D. (2009) The velocity of climate change. *Nature*, **462**, 1052–1055.

Martin, G., Devictor, V., Motard, E., Machon, N. & Porcher, E. (2019) Short-term climate-induced change in French plant communities. *Biology Letters*, **15**, 20190280.

Menéndez, R., Megías, A.G., Hill, J.K., Braschler, B., Willis, S.G., Collingham, Y., … Thomas, C.D. (2006) Species richness changes lag behind climate change. *Proceedings of the Royal Society B: Biological Sciences*, **273**, 1465–1470.

Nakagawa, S. & Schielzeth, H. (2013) A general and simple method for obtaining R2 from generalized linear mixed-effects models. *Methods in Ecology and Evolution*, **4**, 133–142.

Nicolas, M., Jolivet, C. & Jonard, M. (2014) How monitoring networks contribute to the understanding and to the management of soil and forest ecosystems? *Revue forestière française*.

Olofsson, J., Oksanen, L., Callaghan, T., Hulme, P.E., Oksanen, T. & Suominen, O. (2009) Herbivores inhibit climate-driven shrub expansion on the tundra. *Global Change Biology*, **15**, 2681–2693.

Pecl, G.T., Araújo, M.B., Bell, J.D., Blanchard, J., Bonebrake, T.C., Chen, I.-C., … Williams, S.E. (2017) Biodiversity redistribution under climate change: Impacts on ecosystems and human well-being. *Science (New York, N.Y.)*, **355**, eaai9214.

Pebesma, E. (2018) Simple Features for R: Standardized Support for Spatial Vector Data. *The R Journal*, 10, 439–446.

Perring, M.P., Bernhardt-Römermann, M., Baeten, L., Midolo, G., Blondeel, H., Depauw, L., … Verheyen, K. (2018) Global environmental change effects on plant community composition trajectories depend upon management legacies. *Global Change Biology*, **24**, 1722–1740.

Pinheiro, J., Bates, D., DebRoy, S., Sarkar, D. & R Core Team (2019) nlme: Linear and Nonlinear Mixed Effects Models.

Post, E. & Pedersen, C. (2008) Opposing plant community responses to warming with and without herbivores. *Proceedings of the National Academy of Sciences of the United States of America*, **105**, 12353–12358.

R Core Team (2019) R: A Language and Environment for Statistical Computing.

Savage, J. & Vellend, M. (2015) Elevational shifts, biotic homogenization and time lags in vegetation change during 40 years of climate warming. *Ecography*, **38**, 546–555.

Schielzeth, H. (2010) Simple means to improve the interpretability of regression coefficients. *Methods in Ecology and Evolution*, **1**, 103–113.

Stevens, J.T., Safford, H.D., Harrison, S. & Latimer, A.M. (2015) Forest disturbance accelerates thermophilization of understory plant communities. *Journal of Ecology*, **103**, 1253–1263.

Tutin, T.G., Heywood, V.H., Burges, N.A., Valentine, D.H., Walters, S.M. & Webb, D.A. (2001) Flora Europaea 5 Volume Set and CD-ROM Pack.

Ulrich, E. (1995) Le réseau RENECOFOR: objectifs et réalisation. *Revue forestière française*.

Vanderwel, M.C. & Purves, D.W. (2014) How do disturbances and environmental heterogeneity affect the pace of forest distribution shifts under climate change? *Ecography*, **37**, 10–20.

Vuorinen, K.E.M., Kolstad, A.L., De Vriendt, L., Austrheim, G., Tremblay, J.P., Solberg, E.J. & Speed, J.D.M. (2020) Cool as a moose: How can browsing counteract climate warming effects across boreal forest ecosystems? *Ecology*, **101**, 1–10.

Walther, G.-R. (2010) Community and ecosystem responses to recent climate change. *Philosophical Transactions of the Royal Society B: Biological Sciences*, **365**, 2019–2024.

Wickham, H. (2016) ggplot2: Elegant Graphics for Data Analysis, Springer-Verlag New York.

Wickham, H., François, R., Henry, L. & Müller, K. (2019) dplyr: A Grammar of Data Manipulation.

Wilke, C.O. (2019) cowplot: Streamlined Plot Theme and Plot Annotations for "ggplot2."

Williams, J.J., Bates, A.E. & Newbold, T. (2020) Human-dominated land uses favour species affiliated with more extreme climates, especially in the tropics. *Ecography*, **43**, 391–405.

Zellweger, F., Coomes, D., Lenoir, J., Depauw, L., Maes, S.L., Wulf, M., … De Frenne, P. (2019) Seasonal drivers of understorey temperature buffering in temperate deciduous forests across Europe. *Global Ecology and Biogeography*, geb.12991.

786 Zellweger, F., De Frenne, P., Lenoir, J., Vangansbeke, P., Verheyen, K., Bernhardt-
787 Römermann, M., … Coomes, D. (2020) Forest microclimate dynamics drive plant
788 responses to warming. *Science*, **368**, 772 LP–775.

789 Zuur, A., Ieno, E.N. & Graham, S.M. (2007) *Analyzing Ecological Data*, Springer-
790 Verlag New York.

791

Data Accessibility Statement

Datasets on CTI values are provided in Supporting Information, and will be archived in an appropriate public repository after the process of review and acceptance of the manuscript.

Figures

List and captions

Figure 1.
Workflow implemented in the study. The 102 plots of the RENECOFOR network are mapped, and the two datasets used in our analyses are represented in color (in red and blue for the five-year and yearly datasets, respectively). Analyses of temporal trends in mean annual temperature (MAT) and the community temperature index (CTI) and factors contributing to the lag between MAT and CTI (MAT-CTI) are conducted on the two datasets separately. For more details, see the Materials and Methods section.

Figure 2.
Temporal trends for mean annual temperature (MAT) and the community temperature index (CTI) in (a) the five-year dataset from 1995 to 2015 and (b) the yearly dataset from 1995 to 2017. Linear trends (dashed lines) with standard errors (ribbons) of estimated MAT or CTI values are shown. For CTI, the values for exclosure or enclosure are plotted separately. Observed values for temperatures (MAT or CTI) are represented with their associated standard errors and symbol sizes are proportional to sample size (number of plots).

Figure 3.
Coefficient estimates and 95% confidence intervals extracted from linear mixed-effects models testing the relative contribution of several potential abiotic and biotic determinants on the magnitude and direction of the lag between mean annual

temperature (MAT) and the community temperature index (CTI) values in (a) the five-year dataset and (b) yearly dataset. Points (with 95% confidence intervals) represent the standardized mean coefficients averaged from the selected models (Δ AICc < 2) in the model-averaging procedure. Colors show the magnitude and significance of effects (red: significant amplification of the lag; blue: significant mitigation of the lag; light grey: non-significant).

Figure 4.

Plots of partial residuals illustrating the contribution of three factors in explaining the magnitude and direction of the lag between mean annual temperature (MAT) and the community temperature index (CTI) for the yearly dataset. These plots indicate the effects of each of the three factors when all others factors in the model are accounted for and set to their mean value for quantitative variables. Qualitative variables were set to deciduous stands and to outside the fence area here. The factors (a) 'Years', (b) 'Stand Basal Area' and (c) 'Stand Age in 1995' were extracted from the best model (in the model-averaging procedure) explaining the lagged responses of forest plant communities in the yearly dataset. Solid lines and ribbons represent the linear trend and associated standard errors, respectively.

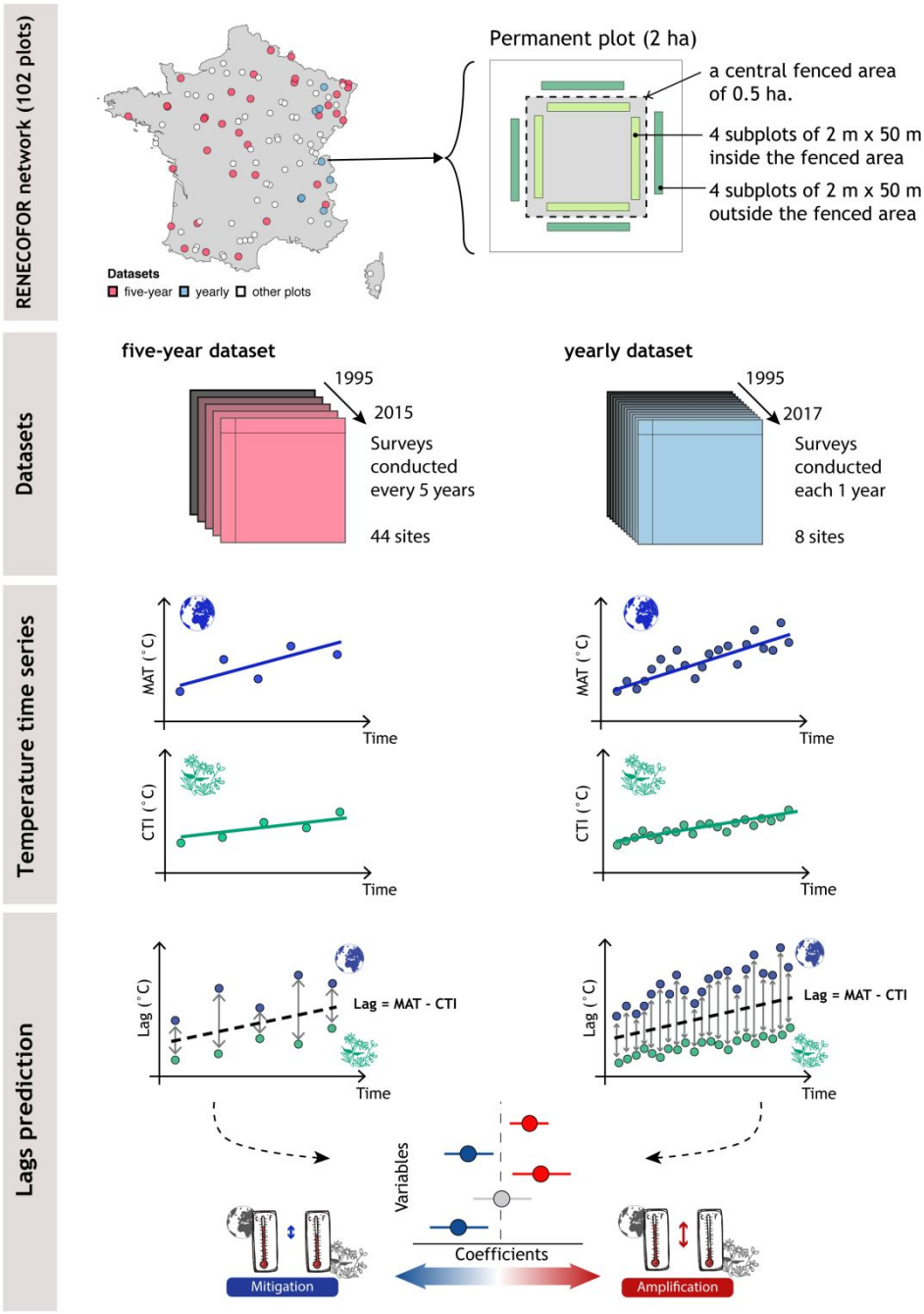
RENECOFOR network (102 plots)
Permanent plot (2 ha)
a central fenced area of 0.5 ha.
4 subplots of 2 m x 50 m inside the fenced area
4 subplots of 2 m x 50 m outside the fenced area
Datasets
five-year yearly other plots
Datasets
five-year dataset
1995
2015
Surveys conducted every 5 years
44 sites
yearly dataset
1995
2017
Surveys conducted each 1 year
8 sites
Temperature time series
MAT (°C)
Time
CTI (°C)
Time
Lags prediction
Lag (°C)
Lag = MAT - CTI
Time
Variables
Coefficients
Mitigation
Amplification

Figure 1.

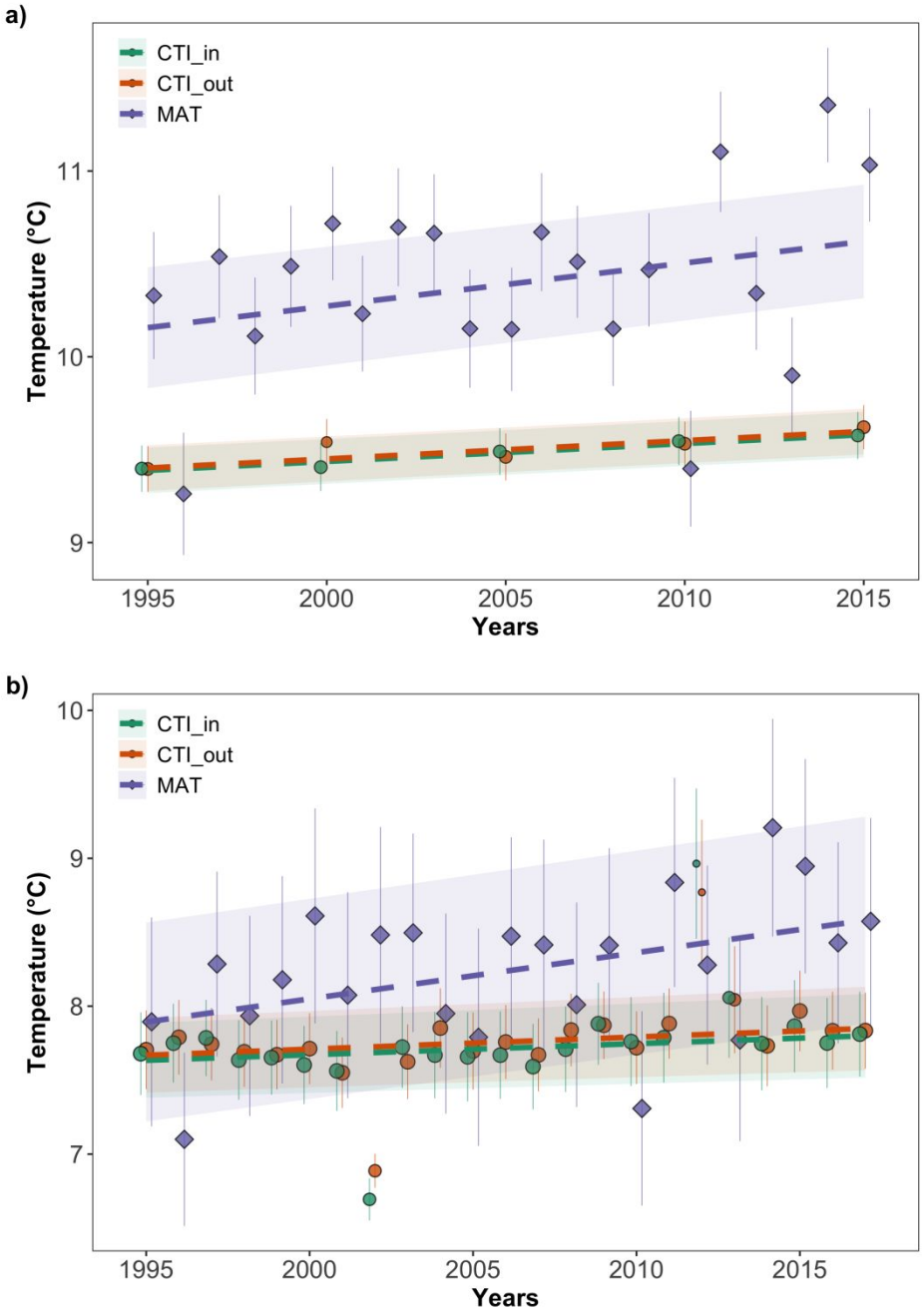

840

841 **Figure 2.**

842

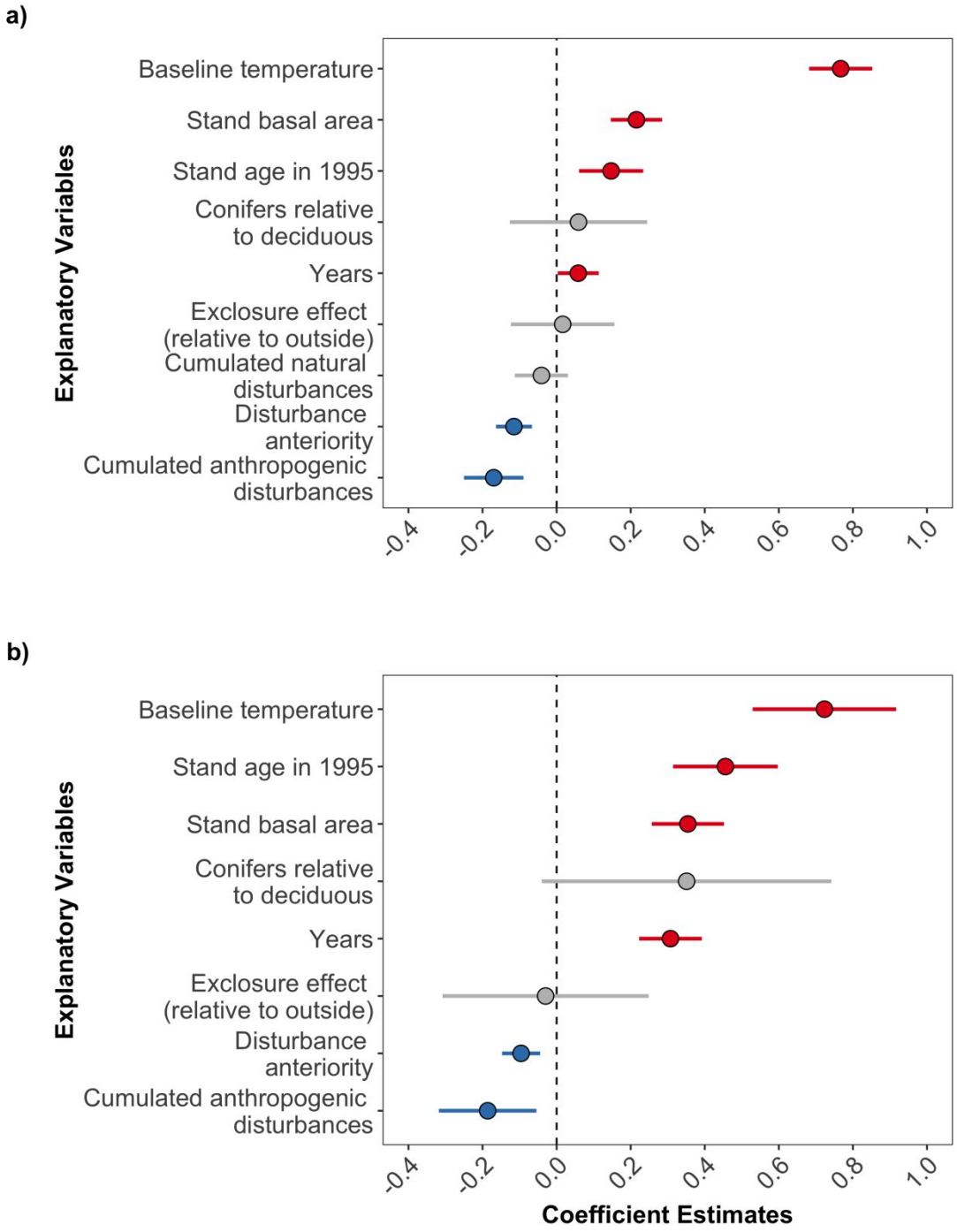

843

844 **Figure 3.**

845

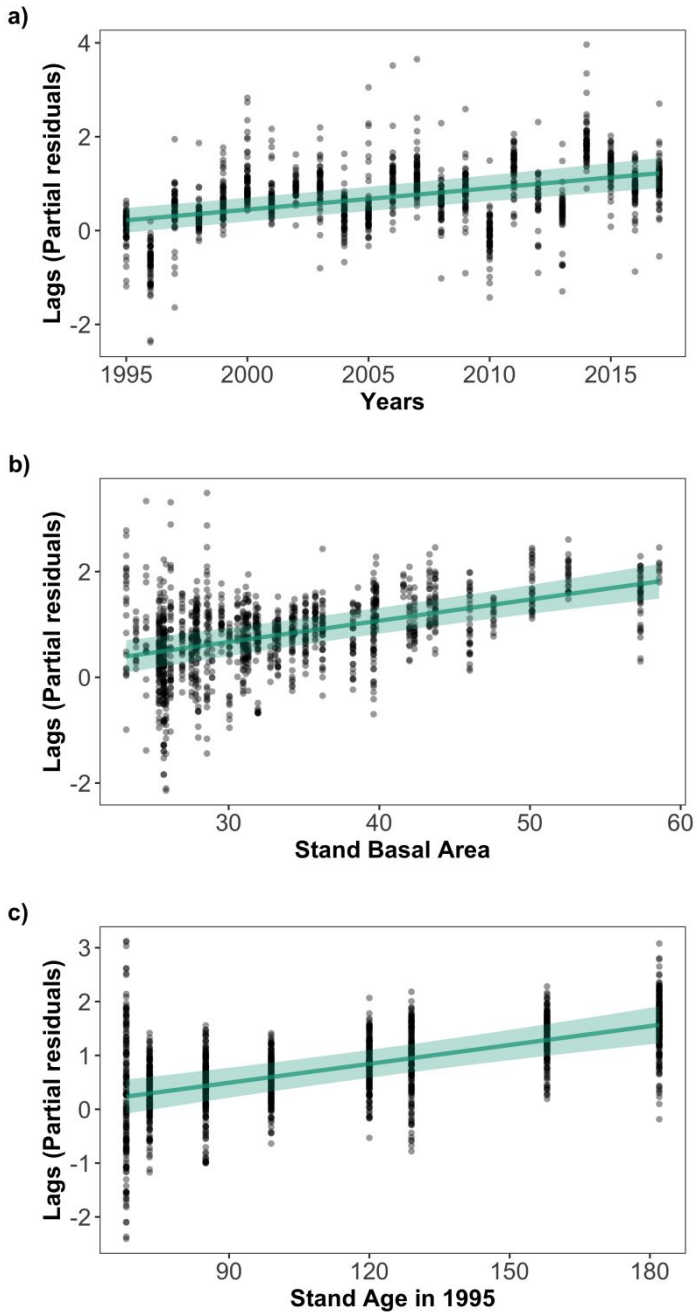

846

847 **Figure 4.**

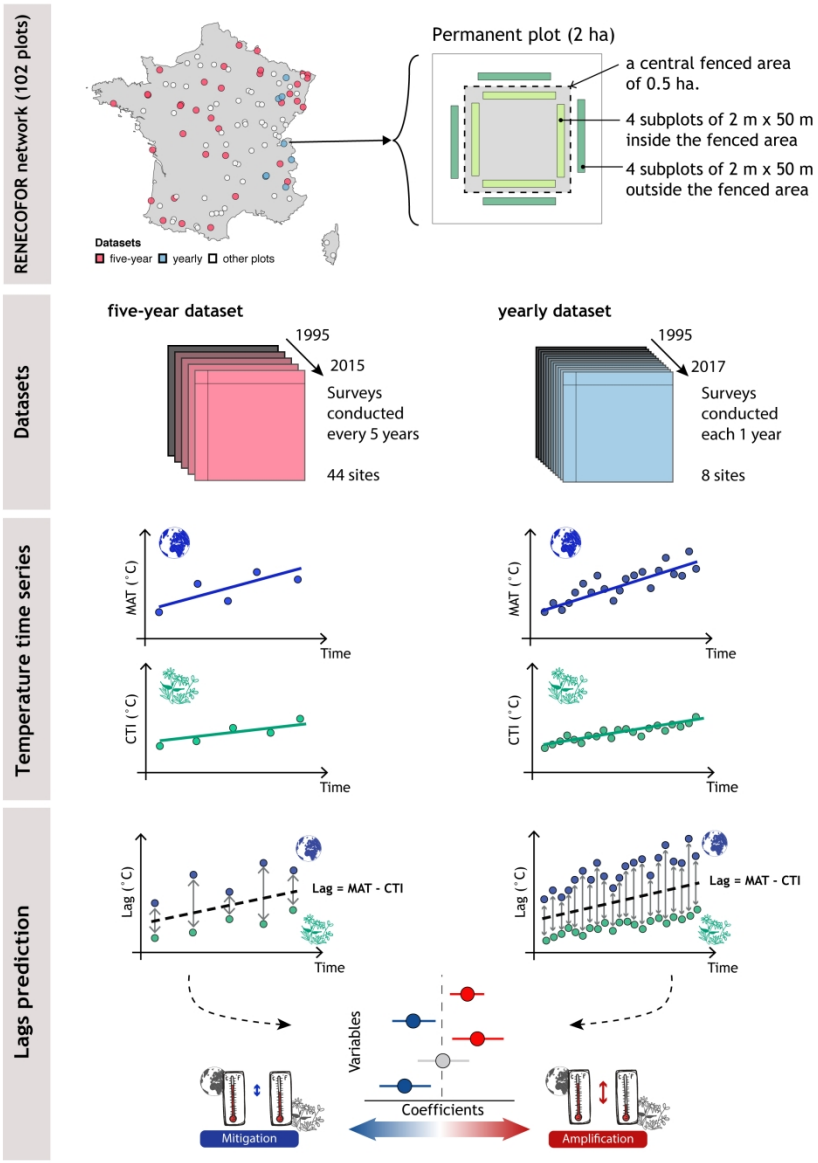

Figure 1. Workflow implemented in the study. The 102 plots of the RENECOFOR network are mapped, and the two datasets used in our analyses are represented in color (in red and blue for the five-year and yearly datasets, respectively). Analyses of temporal trends in mean annual temperature (MAT) and the community temperature index (CTI) and factors contributing to the lag between MAT and CTI (MAT-CTI) are conducted on the two datasets separately. For more details, see the Materials and Methods section.

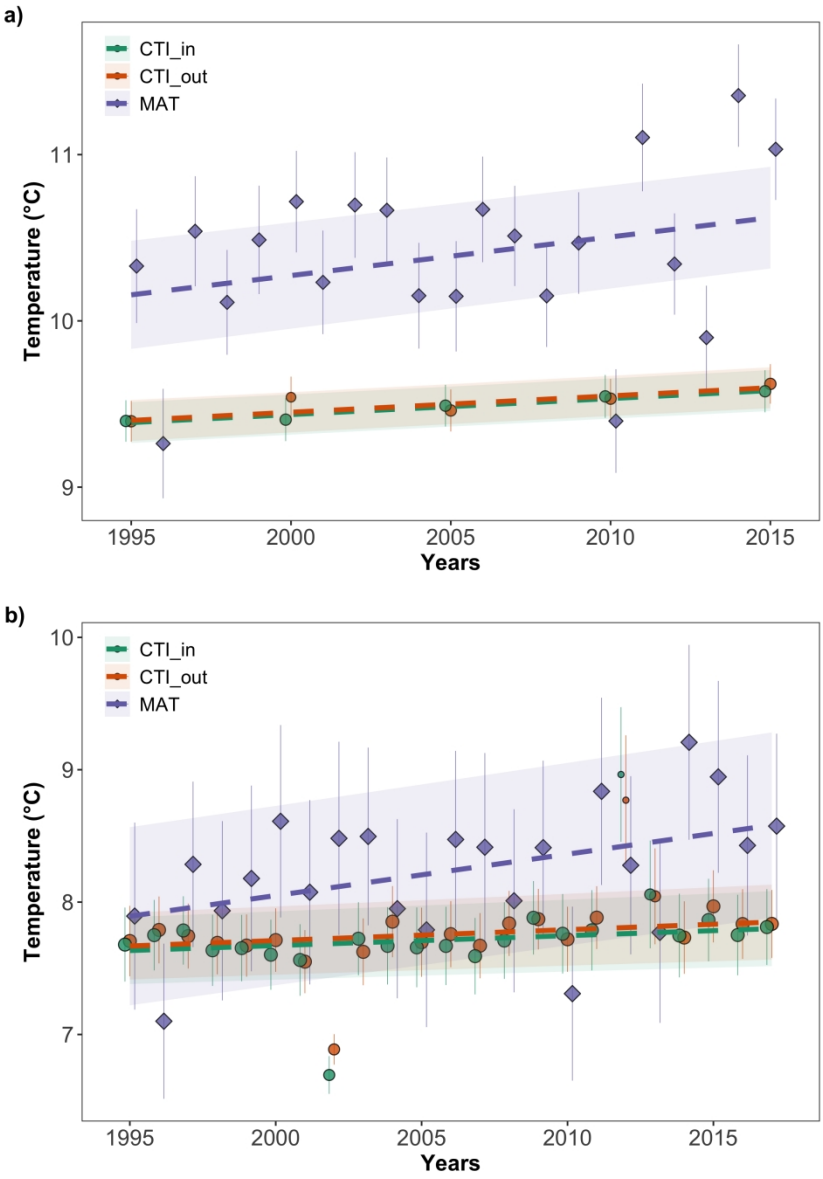

Figure 2. Temporal trends for mean annual temperature (MAT) and the community temperature index (CTI) in (a) the five-year dataset from 1995 to 2015 and (b) the yearly dataset from 1995 to 2017. Linear trends (dashed lines) with standard errors (ribbons) of estimated MAT or CTI values are shown. For CTI, the values for exclosure or enclosure are plotted separately. Observed values for temperatures (MAT or CTI) are represented with their associated standard errors and symbol sizes are proportional to sample size (number of plots).

926x1296mm (72 x 72 DPI)

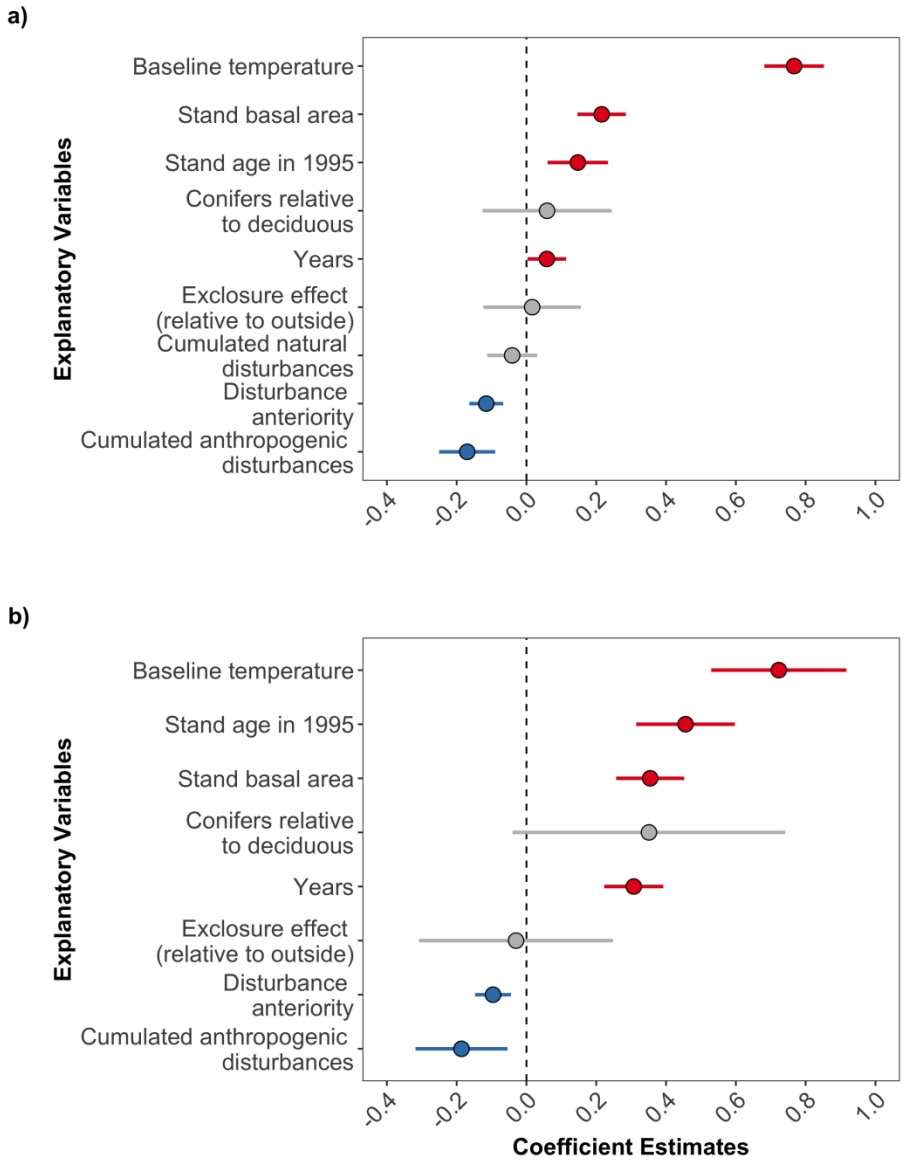

Figure 3. Coefficient estimates and 95% confidence intervals extracted from linear mixed-effects models testing the relative contribution of several potential abiotic and biotic determinants on the magnitude and direction of the lag between mean annual temperature (MAT) and the community temperature index (CTI) values in (a) the five-year dataset and (b) yearly dataset. Points (with 95% confidence intervals) represent the standardized mean coefficients averaged from the selected models (ΔAICc < 2) in the model-averaging procedure. Colors show the magnitude and significance of effects (red: significant amplification of the lag; blue: significant mitigation of the lag; light grey: non-significant).

987x1234mm (72 x 72 DPI)

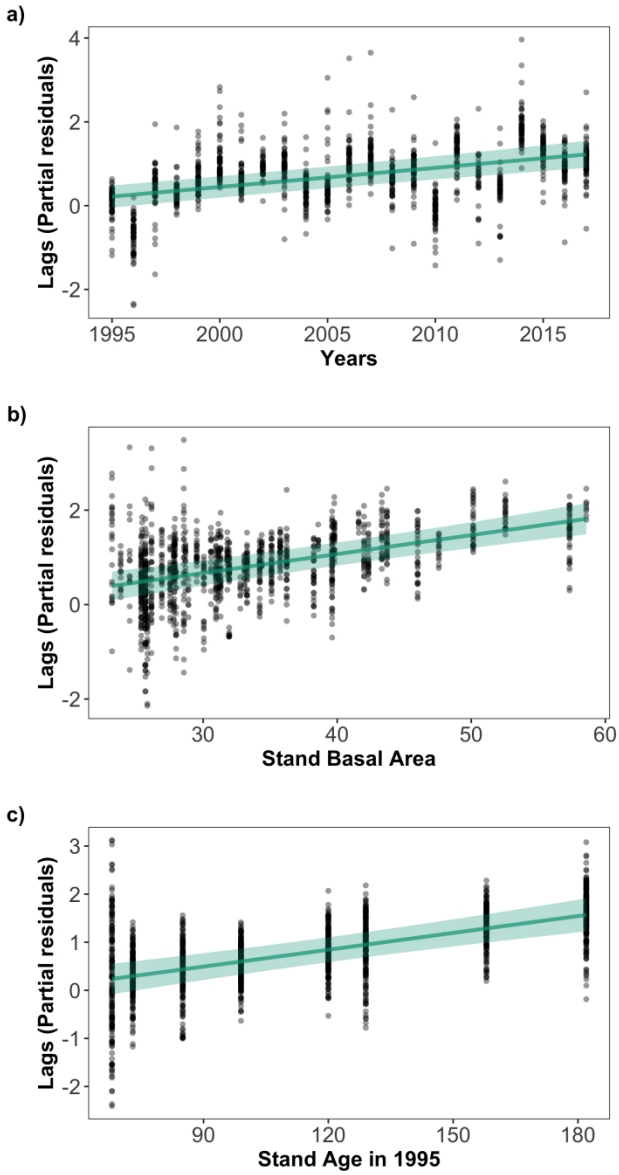

Figure 4. Plots of partial residuals illustrating the contribution of three factors in explaining the magnitude and direction of the lag between mean annual temperature (MAT) and the community temperature index (CTI) for the yearly dataset. These plots indicate the effects of each of the three factors when all others factors in the model are accounted for and set to their mean value for quantitative variables. Qualitative variables were set to deciduous stands and to outside the fence area here. The factors (a) 'Years', (b) 'Stand Basal Area' and (c) 'Stand Age in 1995' were extracted from the best model (in the model-averaging procedure) explaining the lagged responses of forest plant communities in the yearly dataset. Solid lines and ribbons represent the linear trend and associated standard errors, respectively.

740x1358mm (72 x 72 DPI)

Supplementary Information

Title:

1. **The climatic debt is growing in the understory of temperate forests:** stand characteristics matter

2. **Running title:** Explaining the climatic debt of temperate forests

List of appendices (figures and tables):

1. **App. Fig. 1** | Location of the monitored plots throughout France and the time-sequence of resurveys for each plot.

2. **App. Fig. 2** | Comparison between different dataset sources for macroclimate temperature time series.

3. **App. Fig. 3** | Trends in mean annual temperatures anomalies from 1958 to 2017 across the 44 study plots.

4. **App. Fig. 4** | Construction of the Community Temperature Indices (CTIs) and the transfer function.

5. **App. Fig. 5** | Information used to construct the transfer function for calculating CTI values.

6. **App. Fig. 6** | Illustration of the indices created to account for disturbance and forest management.

7. **App. Fig. 7** | Plots of disturbance and forest management indices with data from each studied plot.

8. **App. Fig. 8** | Correlation matrix plots for explanatory variables used in our models.

9. **App. Fig. 9** | Partial residuals plots for variables explaning lags in the best model in the five-year dataset.

10. **App. Fig. 10** | Partial residuals plots for variables explaning lags in the best model in the yearly dataset.

11. **App. Fig. 11** | Average of species richness over time (a), number of species gained or lost between survey years (b), and mean of IV for Temperature over time in group of species gained or lost between survey years (c).

12. **App. Fig. 12** | Trends over time of species richness within each class of IV for Temperature, Light and Nitrogen.

13. **App. Table 1** | Informations on sites characteristics.

14. **App. Table 2** | List of 751 forest species found in the herbaceous layer in our study.

15. **App. Tables 3 & 4** | Results of the model-averaging procedures and selected models.

16. **App. Table 5** | Review of some scientific publications studying the thermophilization rates (expressed in °C/decade) in different ecosystems and taxonomic groups.

Captions:

App. Figure 1. Location of the monitored plots throughout France (a) and the time-sequence plot for the repeated surveys (b). The two datasets are distinguished by color (in black and light blue for the five-year dataset and yearly dataset, respectively). Seasonal relevés are represented by different symbols (∘, Spring; +, Summer; ×, Autumn) and grouped by year. Labels refer to the names of plots in the RENECOFOR network. The baseline TerraClimate temperature conditions over the 1960–1990 period is used as background raster.

App. Figure 2. Comparisons between three sources of time-series for macroclimate temperatures (TerraClimate, CHELSA and local meteorological stations). For comparisons, only 13 sites from the RENECOFOR network were used because they had local meteorological stations nearby. a) Location of the 13 sites from the RENECOFOR network used for comparisons. b) Time-series of macroclimate temperatures provided by TerraClimate, CHELSA, and the meteorological stations. Shaded ribbon (in grey) and dotted line show the beginning of vegetation surveys in the RENECOFOR monitoring program.

App. Figure 3. Trends in mean annual temperatures anomalies from 1958 to 2017 in the 44 permanent plots studied. Temperature anomalies are computed for each permanent plot as the difference between yearly temperatures and the mean temperature over the period 1958–2017. The black line depicts a 5-year moving average of MAT. Mean of temperature anomalies and standard errors are

represented, red and blue colors correspond to positive and negative values, respectively. Shaded ribbon in grey and arrow show the beginning of vegetation surveys in the RENECOFOR monitoring program.

App. Figure 4. Workflow conducted to calculate the Community Temperature Indices (CTIs) through the transfer function.

App. Figure 5. Supporting information for the construction of Community Temperature Indices (CTIs) using the transfer function.

a) Venn diagram depicting the number of taxa recorded in the CATMINAT and EcoPlant databases for species indicator value of temperature. Our dataset includes a total of 877 taxa (all strata of vegetation combined).

b) Relationship between the IVs of temperature of CATMINAT and EcoPlant at the species level.

c) Map of the sites where the NFI floristic surveys have been performed, and which have been used to model the transfer function.

d) Hexagonal binning plot between the CTIs calculated with CATMINAT and EcoPlant at the community level, and the transfer function fitted to obtain CTI values from CATMINAT in degrees Celsius.

Text details for App. Figure 5 : To infer temperature from plant species assemblages, we used an approach based on Community Temperature Indices (CTIs) with species Indicator Values (IVs), and a transfer function to model the

relationship of two databases : CATMINAT (Julve, 1998) and EcoPlant (Gégout et al., 2005). These two databases were chosen, because CATMINAT contains almost all of species recorded in our dataset and EcoPlant, poorer in species, has the advantage to allow the direct computation of CTI values in degrees Celsius. CATMINAT (Julve, 1998) is based on expert knowledge similarly to Ellenberg IVs (Ellenberg et al., 1992), with temperature preferences of plant species coded along an ordinal scale from cold (1) to warm (9) environments. While the CATMINAT database contains almost all of the species sampled in the RENECOFOR monitoring program (858 out of the 877 species recorded within all strata of vegetation; **App. Fig. 5a**), CTI values estimated with these species IVs are unitless and direct comparisons with macroclimatic temperatures are not possible. On the other hand, EcoPlant allows the computation of CTI values in degrees Celsius. EcoPlant is a phyto-ecological database which provides information about ecological optimum for key variables of forest plant species based on their distribution over the French territory. In EcoPlant, species IV for temperature are expressed in degrees Celsius as they are estimated using logistic regression models based on climatic data from AURELHY dataset for the historical period (1961–1990). Nevertheless, the EcoPlant database covers much less species from our dataset (396 out of 877 species). Therefore, we calibrated a transfer function to transform the unitless CTI values from the CATMINAT database into a CTI value expressed in degrees Celsius. By regressing CTI values from EcoPlant against CTI values from CATMINAT, we can obtain predicted CTI values from CATMINAT expressed in degrees Celsius (see

Lenoir et al., 2013 for a similar approach). To improve the quality of the fit, we used the community level and not directly the species level **App. Fig. 5b-d**).

To construct the transfer function, we processed as follows:

1. We used an independent dataset of floristic surveys gathered from the French National Forest Inventory (NFI) for the 2005–2016 period to calibrate our transfer function. Homogenization procedures were performed to avoid taxonomic and nomenclatural issues between our dataset, the NFI data and the IV databases. We selected only the floristic surveys from NFI performed during the growing season and surveys recording at least 2 species. This yielded a total of 45 379 surveys covering the whole French territory (**App. Fig. 5c**).

2. Then, we computed the CTI values for each floristic survey both with CATMINAT and EcoPlant, using species presence/absence to give the same weight to common and rare species. The relationship between CTI values from the two IV datasets was also analyzed with species abundance and results were similar (Pearson' correlation between occurrence and abundance data = 0.88, t = 386, df = 45 377, P < 0.001).

3. To model the relationship between CTI values from CATMINAT and CTI from EcoPlant, we used a Generalized Additive Model (GAM) with a calibration/training procedure to select the best smoothness parameter λ. The dataset was split into a training set and a test set (i.e. proportion of 70/30,

respectively). The final GAM was adjusted with $\lambda = 6$ (model with the lowest RMSE) and it explained 72.9% of the total deviance (**App. Fig. 5d**).

App. Figure 6. Illustrative examples of the indices created to account for disturbance and forest management. Two cases are presented : a) A site with two anthropogenic events that occurred during several vegetation surveys ; and b) A site with one anthropogenic event and two natural events that occurred during several vegetation surveys. For survey year, we recorded informations about : (i) Cumulated disturb., as the cumulative number of disturbance known in a forest stand since the plot etablishment, whatever its nature (anthropogenic or natural event); (ii) the Type of last event (anthropogenic or natural event); (iii) Anteriority, as the anteriority in year of the last disturbance whatever its nature; (iv) the Cumulated disturb. of anthropogenic events : (v) the Cumulated disturb. of natural events. Only the columns filled in grey were used in our analyses. Anthropogenic events include mainly silvicultural operations such as thinning, logging, tree extraction, cleaning brush and forestry machine passage. Natural events include for example, windfalls and tree uprooting after a storm event.

App. Figure 7. Cumulative number of disturbance events along time for each studied plot. The type of disturbance is distinguished by different symbols, and the anteriority (in years) of the last disturbance is shown by a color scale.

App. Figure 8. Correlation matrix plots between explanatory variables used in our analyses, showing scatterplots, density curves and Pearson correlation coefficients for the explanatory variables tested in the models. 'lags': difference MAT – CTI;

'Years': Year of survey; 'Baseline T°C': the baseline temperature conditions during the 1961–1990 period; 'Age in 1995': Age of forest stand in 1995 (year of the first field campaign); 'Disturb. anterior': Anteriority (in years) of the last disturbance which occurred in the plot ; 'Cum.anthr.disturb.': cumulative sum of the number of annual anthropogenic disturbances; 'Cum.nat.disturb.': cumulative sum of the number of natural disturbances ; 'Basal area': forest stand basal area. See Materials and methods for further details.

App. Figure 9. Partial residuals plots for factors contributing to lags in the best model selected by the model averaging procedure in the five-year dataset. Partial residuals are the residuals that remain after removing the effect of all other covariates in the model.

App. Figure 10. Partial residuals plots for factors contributing to lags in the best model selected by the model averaging procedure in the yearly dataset. Partial residuals are the residuals that remain after removing the effect of all other covariates in the model.

App. Figure 11. Species richness changes over time (a), Number of species gained or lost between survey years (b), and Temporal changes over time for averages of IVs for Temperature within the group of species gained or lost between survey years (c). Points and error bars correspond to the average of values between the 44 studied sites and the standard errors, respectively. For the temporal changes, we compared the species lists between the first survey in 1995 and the later surveys of each plot to identify the pools of species gained and lost between each pair of surveys. In

particular, these two pools are used to calculate temporal β-diversity between two surveys of a given plot (Legendre, 2019). Then, we computed the average of IVs for Temperature within the gained and lost species.

App. Figure 12. Temporal changes over time in species richness within each class of IV for Temperature, Light and Nitrogen (from CATMINAT, Julve, 1998). Each class of IV are detailed in the online version of CATMINAT (http://philippe.julve.pagesperso-orange.fr/catminat.htm). Species richness per classes are expressed in pourcentage of the total species richness in a given plot. Points correspond to the average of species richness between the 44 studied sites, and only significant linear regressions are displayed ($P < 0.05$).

App. Table 1 Informations on sites characteristics detailing the name of RENECOFOR plots, the dominant tree species in the forest stands, the altitude, the geographical coordinates (latitude and longitude in WGS84), and the dataset(s) in which they occurred (see Materials and Methods for details on the yearly or five-year datasets).

App. Table 2 List of 751 forest species inventoried in the herbaceous layer. Species retained for analyses are marked with a "1" in the éponymous column.

App. Tables 3 & 4 Results of the model-averaging procedures and selected models for the studyy of the effects of different variables on lag (difference between MAT and CTI). Only the top 20 models are presented. Coefficients of variables were estimated using linear mixed-effects models (LMMs including 'plot' and 'nested

subplots' as random effects) in a model-averaging procedure. All variables were standardized (z-score) to interpret estimates as relative effect sizes. Coefficient estimates for predictor variables, marginal R^2m and conditional R^2c are shown. R^2m and R^2c describe the variation explained by fixed effects only and variation explained by the fixed and random effects, respectively. Only models with ΔAICc values < 2 were used to estimate coefficients.

App. Table 5 Review of some scientific publications studying the thermophilization rates (expressed in °C/decade) in different ecosystems and taxonomic groups.

198 *Appendices:*

a)

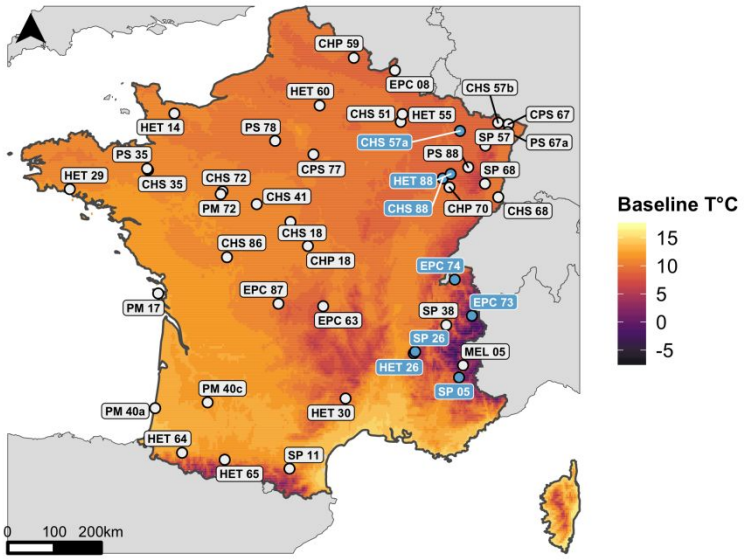

b)

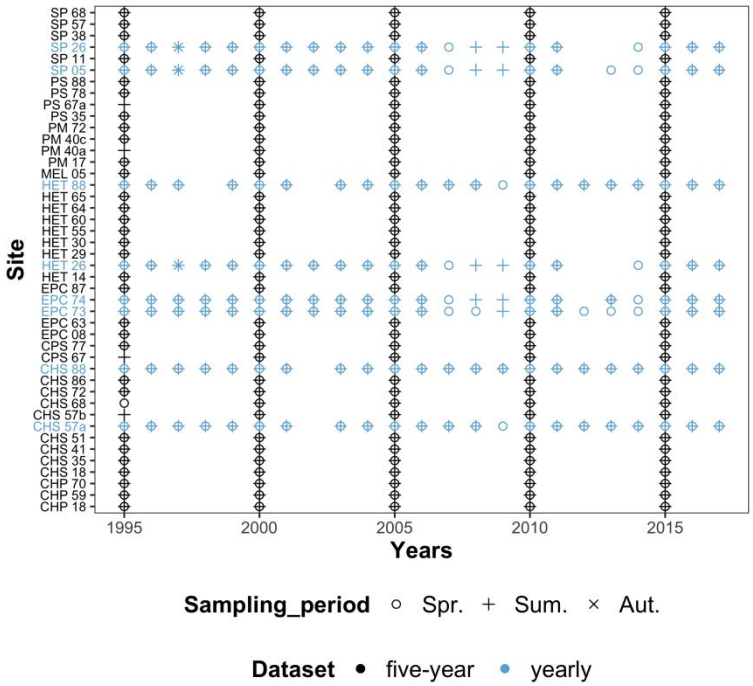

199

200 **App. Figure 1.**

201

a)

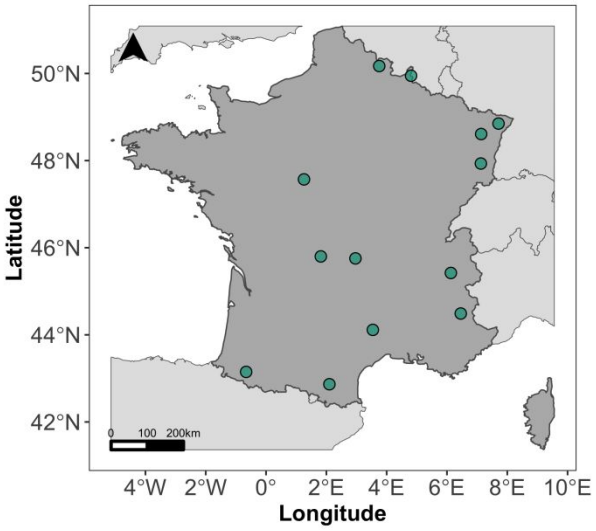

b)

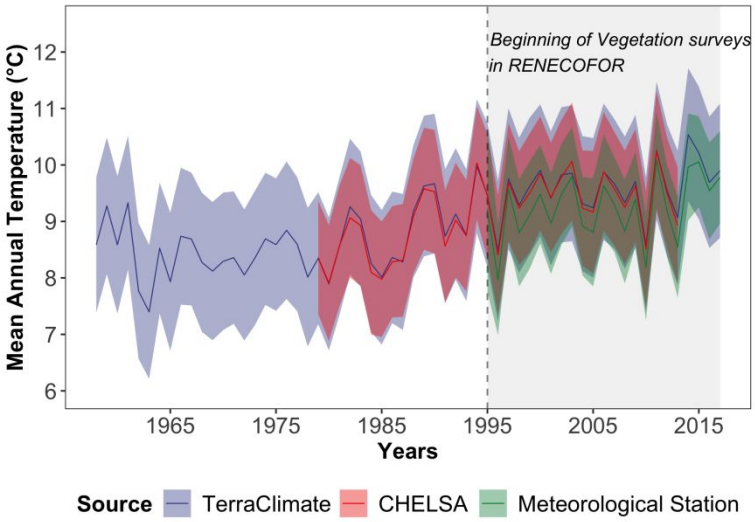

202

203 **App. Figure 2.**

204

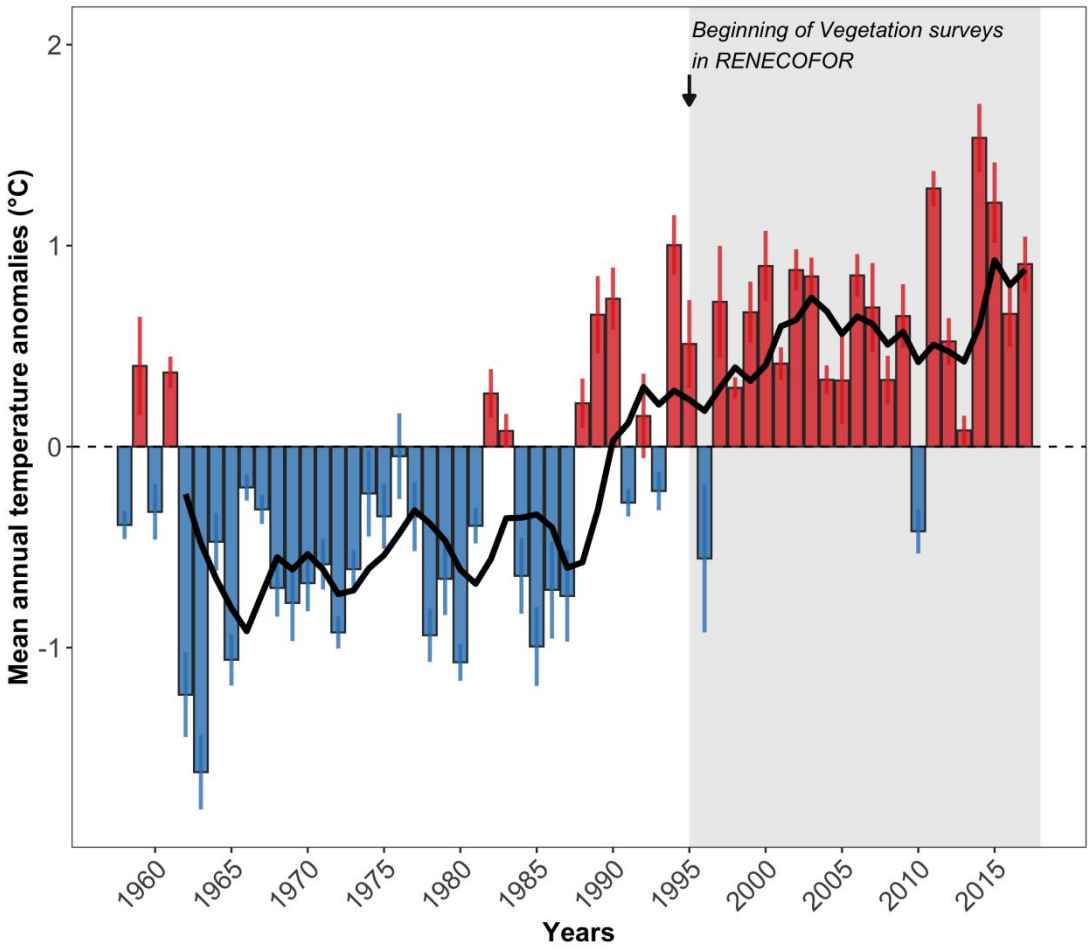

205

206 **App. Figure 3.**

207

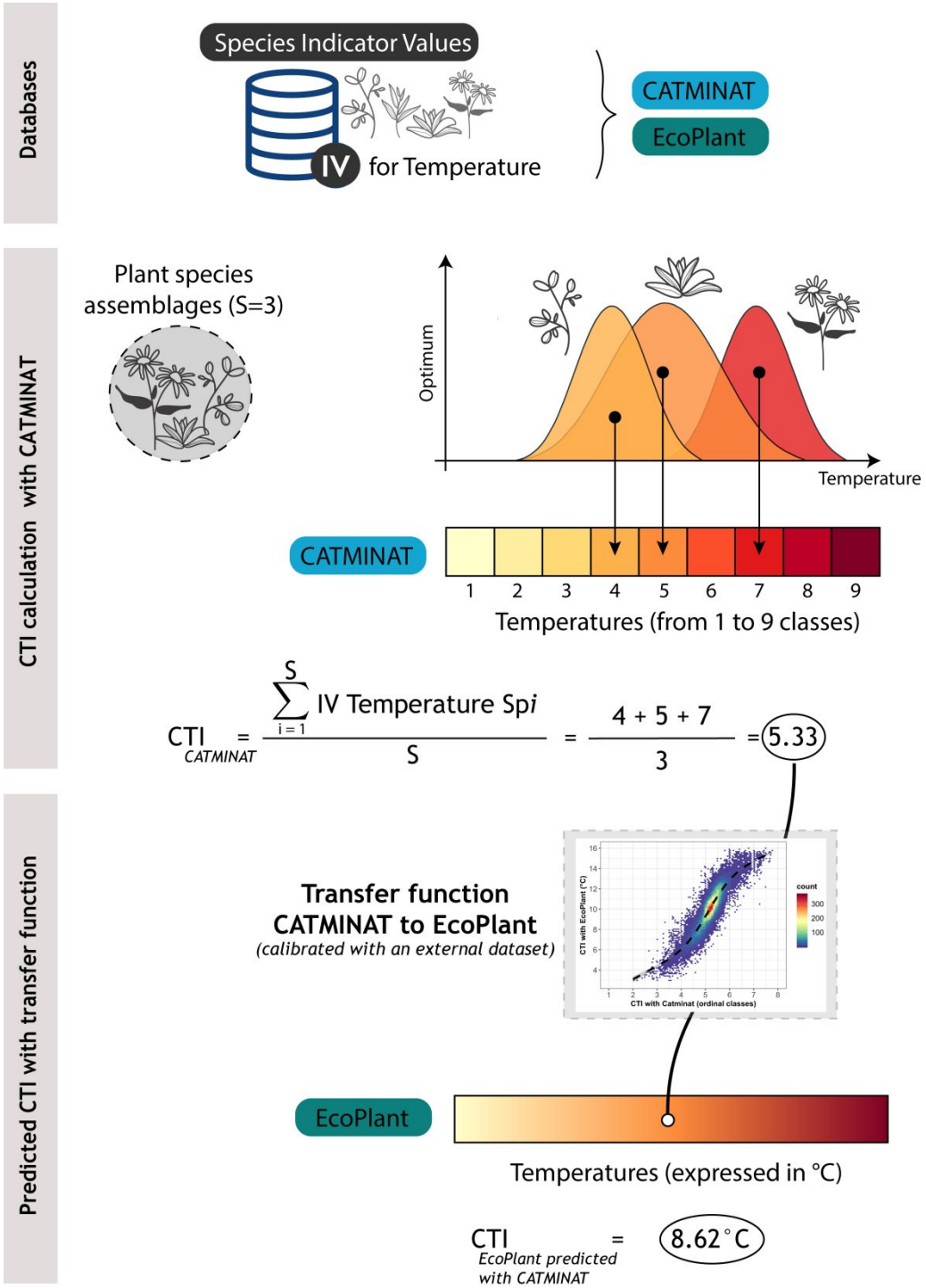
Databases
Species Indicator Values
IV
for Temperature
CATMINAT
EcoPlant
CTI calculation with CATMINAT
Plant species assemblages (S=3)
Optimum
Temperature
CATMINAT
1 2 3 4 5 6 7 8 9
Temperatures (from 1 to 9 classes)
CTI CATMINAT = ∑ i=1 S IV Temperature Spi / S = 4 + 5 + 7 / 3 = 5.33
Predicted CTI with transfer function
Transfer function
CATMINAT to EcoPlant
(calibrated with an external dataset)
CTI with EcoPlant (°C)
CTI with Catminat (ordinal classes)
count
300
200
100
EcoPlant
Temperatures (expressed in °C)
CTI EcoPlant predicted with CATMINAT = 8.62 °C

App. Figure 4.

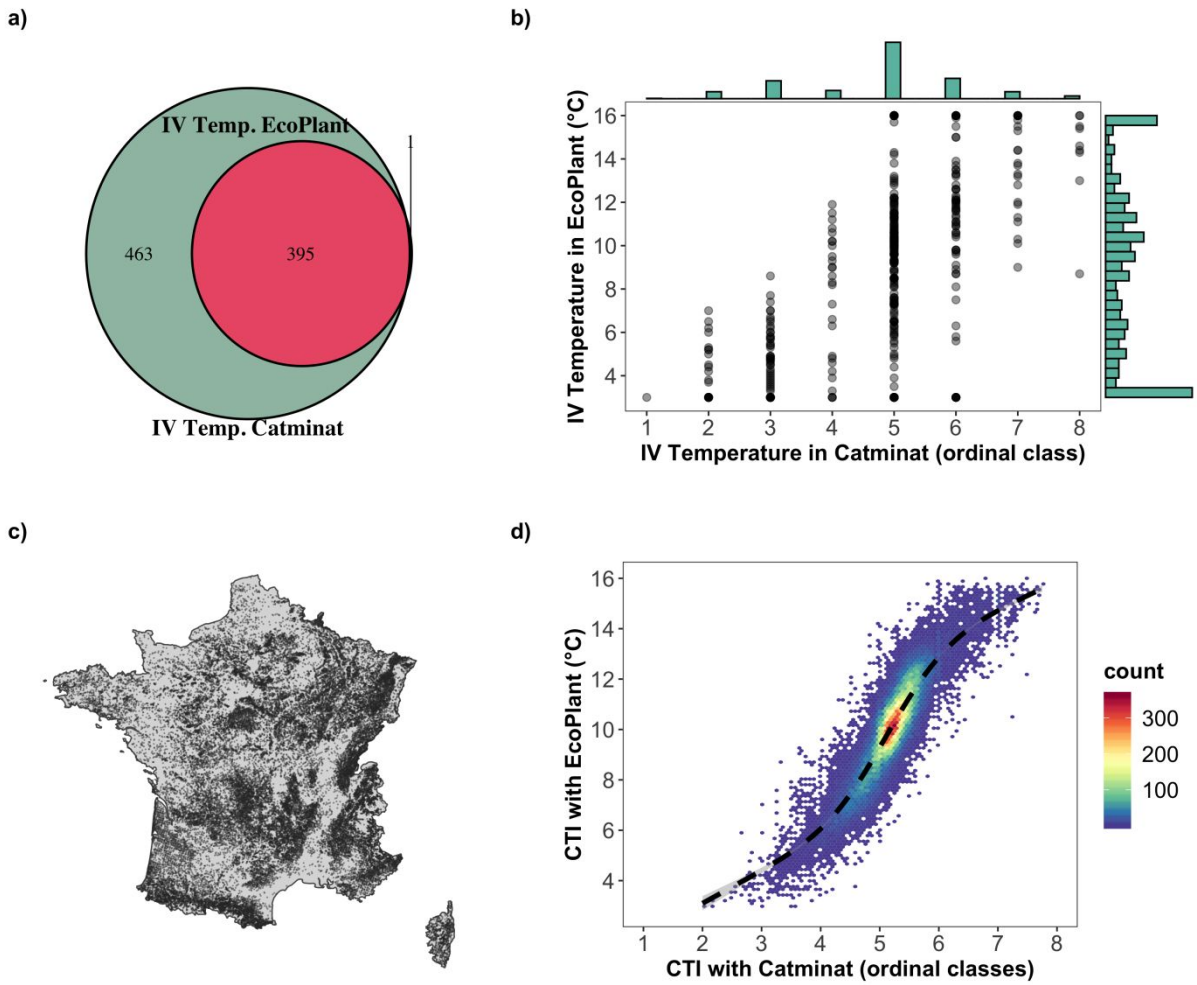

210

211 **App. Figure 5.**

212

Disturbance and Forest management indices

a) Illustrative Case for Anthropogenic events (2 events)

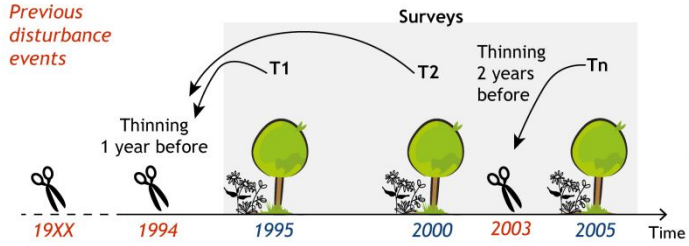

Surveys	(i) Cumulated disturb.	(ii) Type of Last Event	(iii) Anteriority (years)	(iv) Cum. disturb.	(v) Cum. disturb.
T1	2	✂	+ 1	2	0
T2	2	-	+ 6	2	0
Tn	3	✂	+ 2	3	0

b) Illustrative Case for Anthropogenic and Natural events (1 and 2 events, respectively)

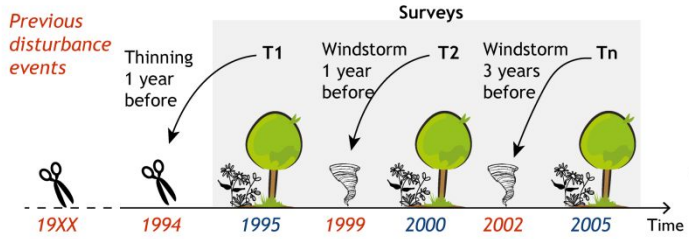

Surveys	(i) Cumulated disturb.	(ii) Type of Last Event	(iii) Anteriority (years)	(iv) Cum. disturb.	(v) Cum. disturb.
T1	2	✂	+ 1	2	0
T2	3	🌪	+ 1	2	1
Tn	4	🌪	+ 3	2	2

213

214 **App. Figure 6.**

215

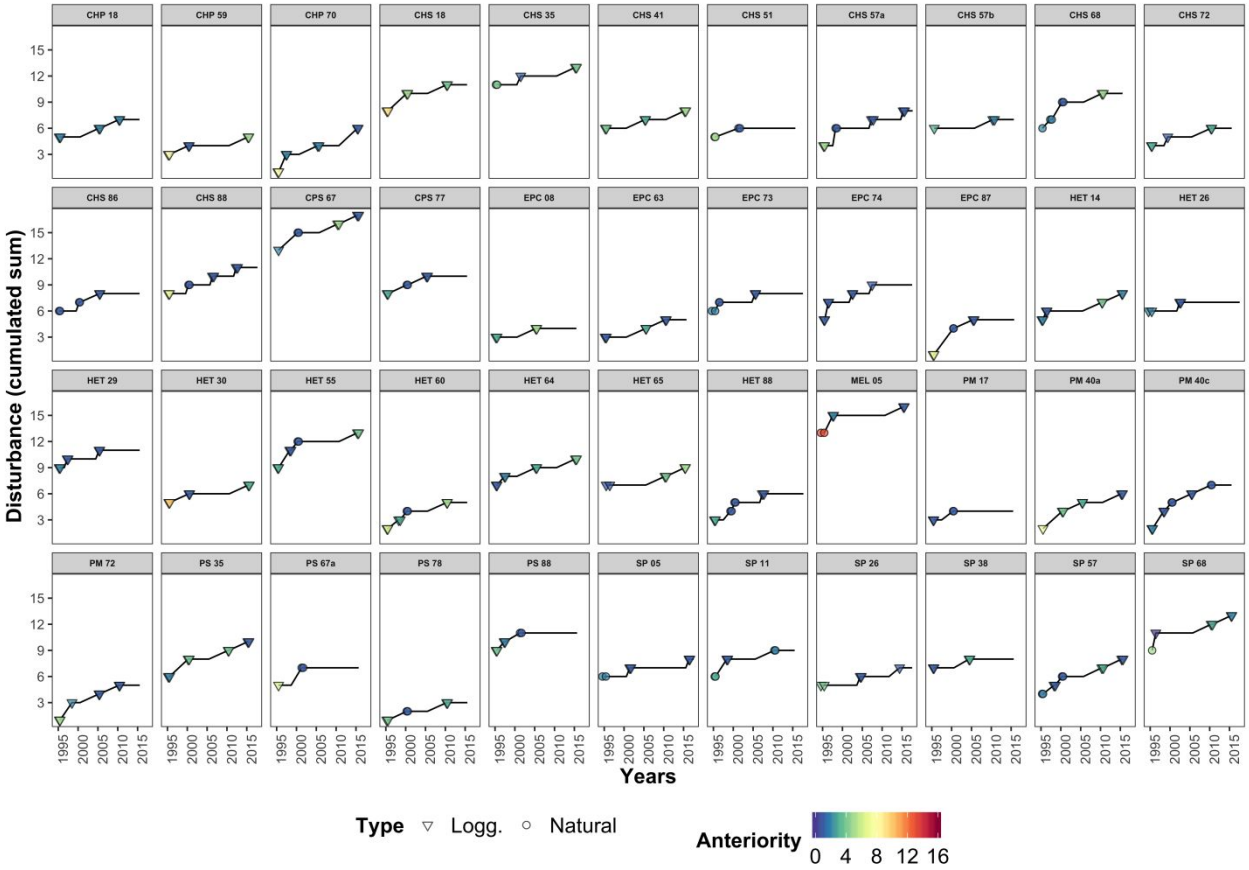

216

217 **App. Figure 7.**

218

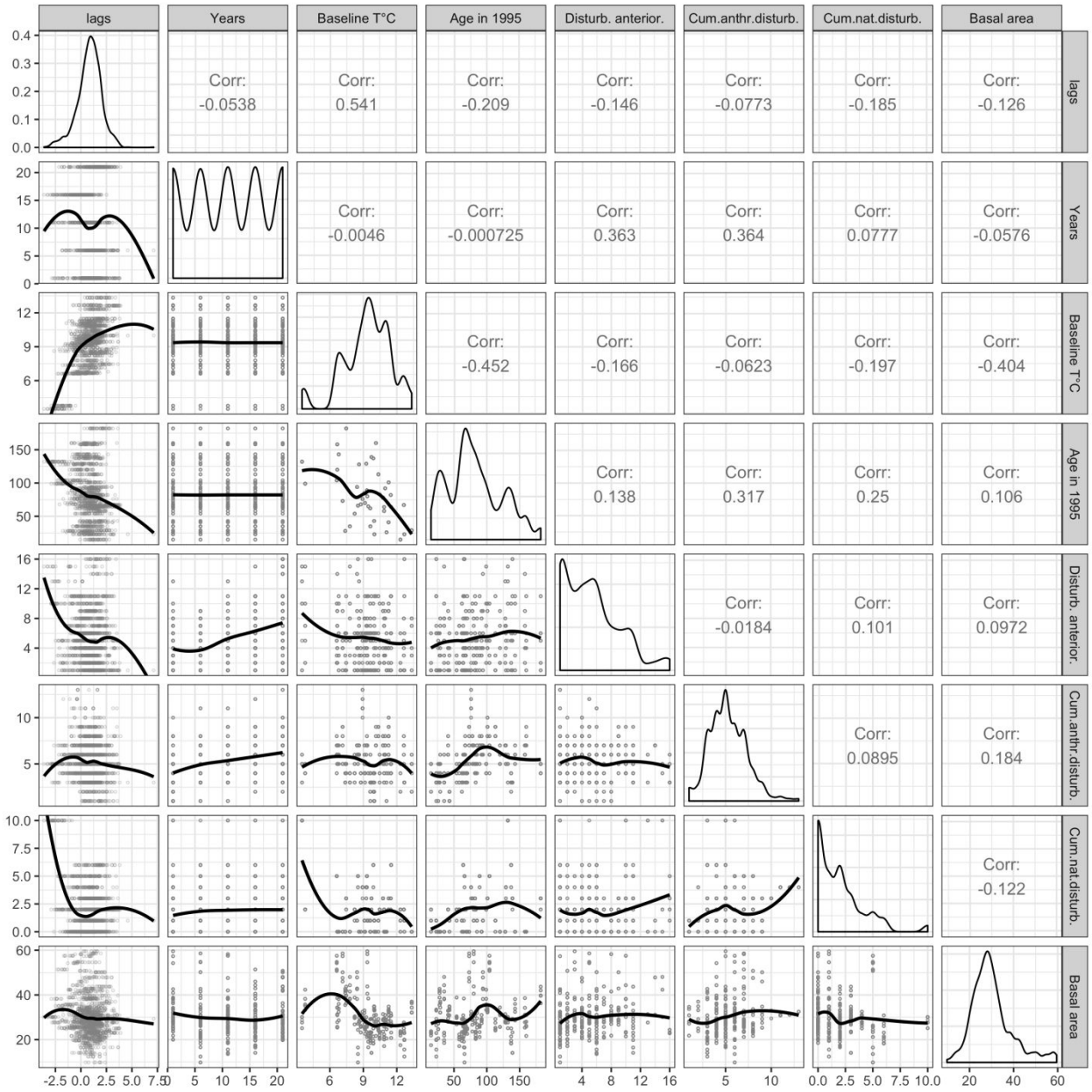
lags
Years
Baseline T°C
Age in 1995
Disturb. anterior.
Cum.anthr.disturb.
Cum.nat.disturb.
Basal area
Corr: -0.0538
Corr: 0.541
Corr: -0.209
Corr: -0.146
Corr: -0.0773
Corr: -0.185
Corr: -0.126
Corr: -0.0046
Corr: -0.000725
Corr: 0.363
Corr: 0.364
Corr: 0.0777
Corr: -0.0576
Corr: -0.452
Corr: -0.166
Corr: -0.0623
Corr: -0.197
Corr: -0.404
Corr: 0.138
Corr: 0.317
Corr: 0.25
Corr: 0.106
Corr: -0.0184
Corr: 0.101
Corr: 0.0972
Corr: 0.0895
Corr: 0.184
Corr: -0.122

App. Figure 8.

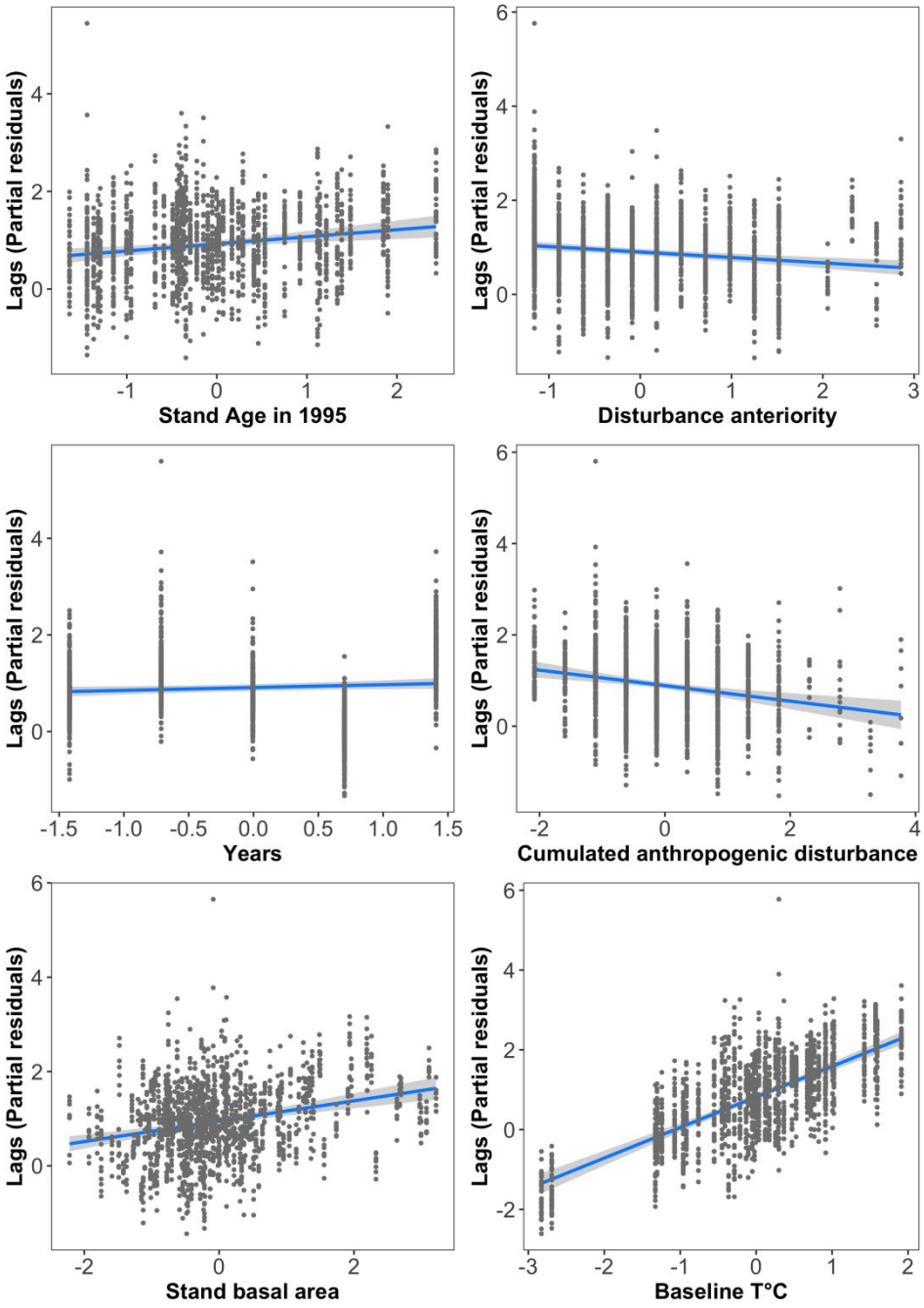
Lags (Partial residuals)
Stand Age in 1995
Disturbance anteriority
Years
Cumulated anthropogenic disturbance
Stand basal area
Baseline T°C

App. Figure 9.

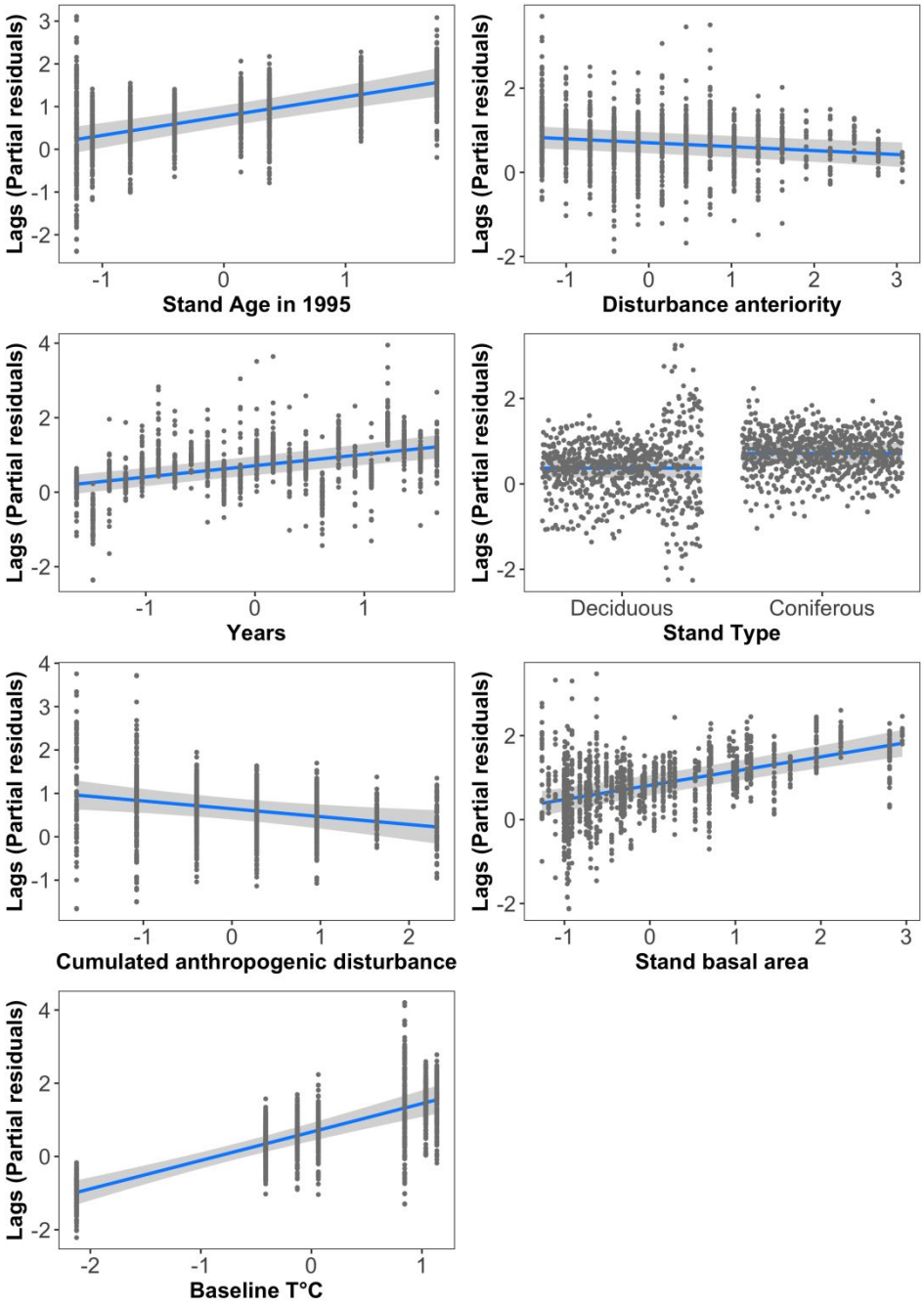

App. Figure 10.

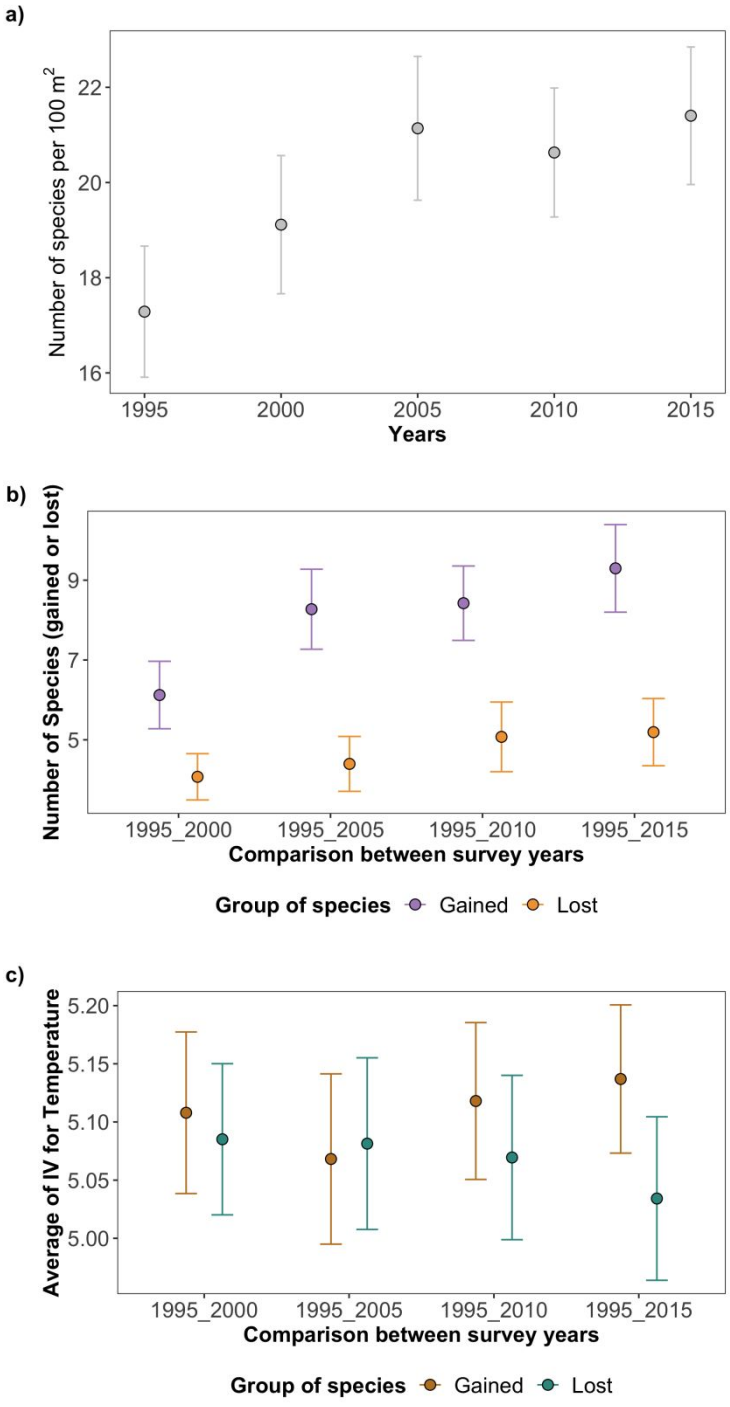

228

229 **App. Figure 11.**

230

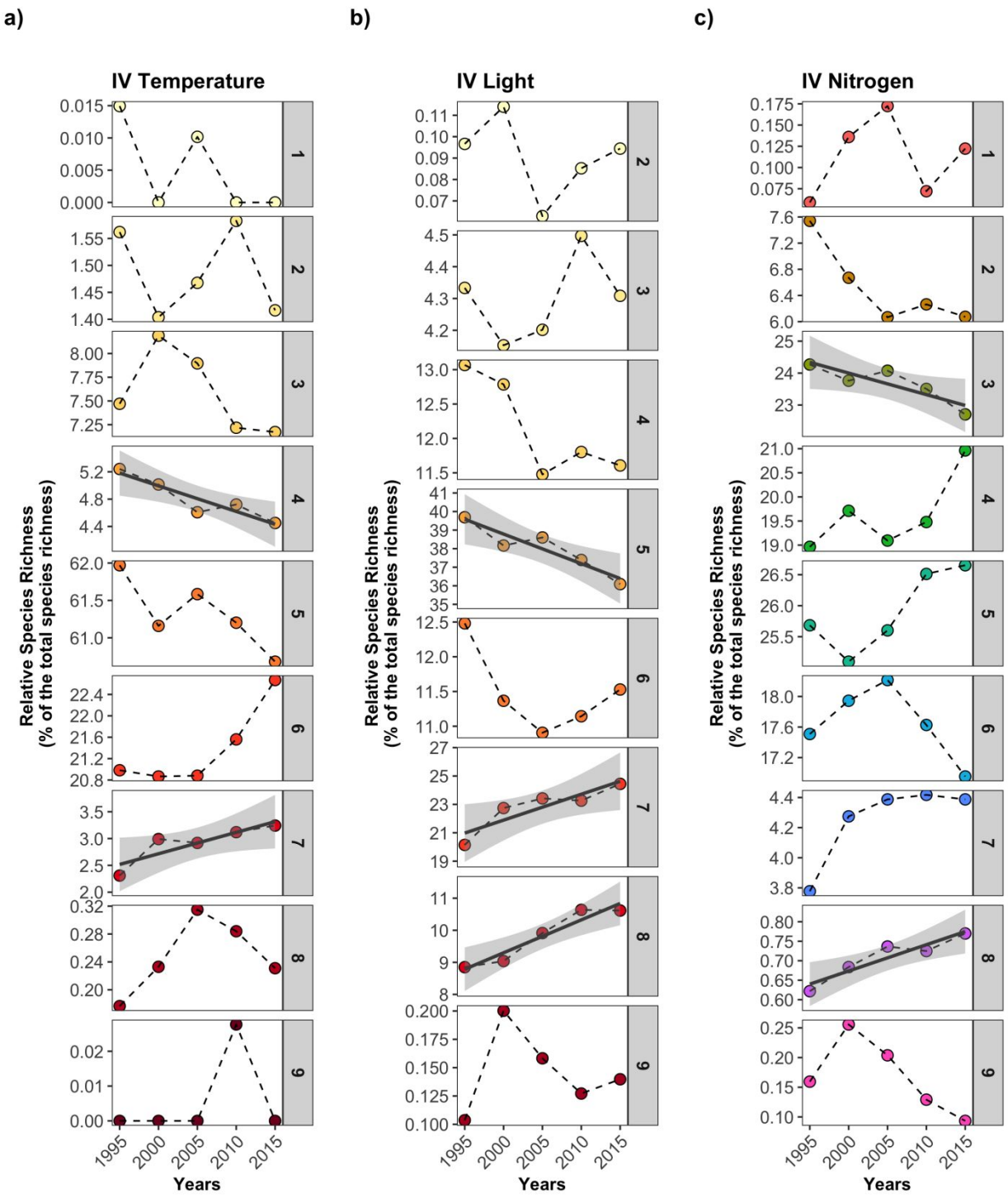

231

232 **App. Figure 12.**

233

App. Table 1 cf. Excel file

App. Table 2 cf. Excel files

App. Tables 3 & 4 cf. Excel files

App. Tables 5 cf. Excel files

References

Ellenberg, H., Weber, H. E., Düll, R., Wirth, V., Werner, W., & Paulißen, D. (1992). Zeigerwerte von Pflanzen in Mitteleuropa. *Scripta Geobotanica*.

Gégout, J. C., Coudun, C., Bailly, G., & Jabiol, B. (2005). EcoPlant: A forest site database linking floristic data with soil and climate variables. *Journal of Vegetation Science*, *16*(2), 257–260. https://doi.org/10.1111/j.1654-1103.2005.tb02363.x

Julve, P. (1998). *Baseflor: Index botanique, écologique et chorologique de la flore de France. Version 2009*. http://philippe.julve.pagesperso-orange.fr/catminat.htm

Legendre, P. (2019). A temporal beta-diversity index to identify sites that have changed in exceptional ways in space–time surveys. *Ecology and Evolution*, *9*(6), 3500–3514. https://doi.org/10.1002/ece3.4984

Lenoir, J., Graae, B. J., Aarrestad, P. A., Alsos, I. G., Armbruster, W. S., Austrheim, G., Bergendorff, C., Birks, H. J. B., Bråthen, K. A., Brunet, J., Bruun, H. H., Dahlberg, C. J., Decocq, G., Diekmann, M., Dynesius, M., Ejrnæs, R., Grytnes, J. A., Hylander, K., Klanderud, K., … Svenning, J. C. (2013). Local temperatures inferred from plant communities suggest strong spatial buffering of climate warming across Northern Europe. *Global Change Biology*, *19*(5), 1470–1481. https://doi.org/10.1111/gcb.12129

Site name	Dominant tree species	Altitude	Latitude_WGS84	Longitude_WGS84	Dataset(s)
CHP 18	Pedunculate oak	175	46.825	2.573	five-year
CHP 59	Pedunculate oak	149	50.171	3.754	five-year
CHP 70	Pedunculate oak	240	47.87	6.211	five-year
CHS 18	Sessile oak	176	47.254	2.125	five-year
CHS 35	Sessile oak	80	48.177	-1.536	five-year
CHS 41	Sessile oak	127	47.569	1.259	five-year
CHS 51	Sessile oak	180	49.032	4.959	five-year
CHS 57a	Sessile oak	315	48.871	6.482	five-year; yearly
CHS 57b	Sessile oak	320	49.016	7.461	five-year
CHS 68	Sessile oak	256	47.693	7.466	five-year
CHS 72	Sessile oak	170	47.796	0.379	five-year
CHS 86	Sessile oak	116	46.626	0.494	five-year
CHS 88	Sessile oak	330	48.026	6.039	five-year; yearly
CPS 67	Sessile or pedunculate oa	350	48.99	7.728	five-year
CPS 77	Sessile or pedunculate oa	80	48.454	2.716	five-year
EPC 08	Norway spurce	480	49.948	4.809	five-year
EPC 63	Norway spurce	950	45.754	2.965	five-year
EPC 73	Norway spurce	1700	45.586	6.789	five-year; yearly
EPC 74	Norway spurce	1200	46.228	6.348	five-year; yearly
EPC 87	Norway spurce	650	45.8	1.816	five-year
HET 14	Beech	90	49.182	-0.858	five-year
HET 26	Beech	1320	44.917	5.294	five-year; yearly
HET 29	Beech	50	47.836	-3.545	five-year
HET 30	Beech	1400	44.114	3.542	five-year
HET 55	Beech	250	49.17	5.004	five-year
HET 60	Beech	138	49.324	2.875	five-year
HET 64	Beech	400	43.149	-0.66	five-year
HET 65	Beech	850	43.026	0.435	five-year
HET 88	Beech	400	48.106	6.244	five-year; yearly
MEL 05	European larch	1850	44.704	6.561	five-year
PM 17	Maritime pine	15	45.982	-1.273	five-year
PM 40a	Maritime pine	27	43.942	-1.352	five-year
PM 40c	Maritime pine	150	44.045	-0.004	five-year
PM 72	Maritime pine	153	47.746	0.333	five-year
PS 35	Scots pine	80	48.201	-1.558	five-year
PS 67a	Scots pine	175	48.85	7.71	five-year
PS 78	Scots pine	170	48.695	1.732	five-year
PS 88	Scots pine	500	48.225	6.695	five-year
SP 05	Silver fir	1360	44.489	6.458	five-year; yearly
SP 11	Silver fir	950	42.866	2.101	five-year
SP 26	Silver fir	1150	44.947	5.331	five-year; yearly
SP 38	Silver fir	1100	45.42	6.13	five-year
SP 57	Silver fir	400	48.609	7.134	five-year
SP 68	Silver fir	680	47.933	7.124	five-year

Species	Species retained for analyses
Abies alba	1
Abies grandis	1
Acer campestre	1
Acer platanoides	1
Acer pseudoplatanus	1
Acer sp.	0
Aceras anthropophorum	1
Achillea macrophylla	1
Achillea millefolium	1
Aconitum lycoctonum subsp. vulparia	1
Aconitum sp.	0
Aconitum variegatum subsp. paniculatum	1
Actaea spicata	1
Adenostyles alliariae	1
Adenostyles alpina	1
Adoxa moschatellina	1
Aegopodium podagraria	1
Aetheorhiza bulbosa	1
Aethusa cynapium subsp. cynapioides	1
Agrimonia eupatoria	1
Agrimonia procera	1
Agrostis agrostiflora	1
Agrostis canina	1
Agrostis capillaris	1
Agrostis curtisii	1
Agrostis sp.	0
Agrostis stolonifera	1
Ajuga pyramidalis	1
Ajuga reptans	1
Ajuga sp.	0
Alchemilla alpina	1
Alchemilla coriacea	1
Alchemilla glaucescens	1
Alchemilla xanthochlora	1
Alliaria petiolata	1
Alnus glutinosa	1
Alnus viridis	1
Alopecurus pratensis	1
Anchusa officinalis	1
Anemone apennina	1
Anemone nemorosa	1
Angelica sylvestris	1
Antennaria dioica	1
Anthoxanthum odoratum	1
Anthoxanthum sp.	0
Anthriscus sylvestris	1
Anthyllis vulneraria	1
Aquilegia vulgaris	1
Arabis brassica	1

Arabis hirsuta	1
Arbutus unedo	1
Arctium nemorosum	1
Arenaria montana	1
Arnica montana	1
Arrhenatherum elatius	1
Arum italicum	1
Arum maculatum	1
Arum sp.	0
Aruncus dioicus	1
Aruncus sp.	0
Asparagus officinalis	1
Asphodelus albus	1
Asplenium trichomanes	1
Asplenium trichomanes-ramosum	1
Astrantia major	1
Athyrium distentifolium	1
Athyrium filix-femina	1
Atropa bella-donna	1
Avena sativa	1
Avena sp.	0
Betula pendula	1
Betula pubescens	1
Betula sp.	0
Blackstonia perfoliata	1
Blechnum spicant	1
Brachypodium pinnatum	1
Brachypodium sp.	0
Brachypodium sylvaticum	1
Briza media	1
Bromus benekenii	1
Bromus ramosus	1
Bromus sp.	0
Buxus sempervirens	1
Calamagrostis epigejos	1
Calamagrostis sp.	0
Calamagrostis varia	1
Calamagrostis villosa	1
Calamintha grandiflora	1
Calamintha sylvatica	1
Callitriche sp.	0
Calluna vulgaris	1
Caltha palustris	1
Campanula barbata	1
Campanula cervicaria	1
Campanula latifolia	1
Campanula rapunculoides	1
Campanula rhomboidalis	1
Campanula rotundifolia	1
Campanula trachelium	1

Cardamine flexuosa	1
Cardamine heptaphylla	1
Cardamine hirsuta	1
Cardamine impatiens	1
Cardamine pentaphyllos	1
Cardamine pratensis	1
Cardamine sp.	0
Carduus carlinifolius	1
Carduus defloratus	1
Carex acutiformis	1
Carex alba	1
Carex arenaria	1
Carex bohemica	1
Carex brizoides	1
Carex caryophyllea	1
Carex curta	1
Carex demissa	1
Carex digitata	1
Carex divulsa	1
Carex echinata	1
Carex ferruginea subsp. australpina	1
Carex flacca	1
Carex flava	1
Carex hallerana	1
Carex hirta	1
Carex laevigata	1
Carex montana	1
Carex muricata	1
Carex muricata subsp. lamprocarpa	1
Carex ornithopoda	1
Carex ovalis	1
Carex pallescens	1
Carex panicea	1
Carex pendula	1
Carex pilosa	1
Carex pilulifera	1
Carex remota	1
Carex sp.	0
Carex strigosa	1
Carex sylvatica	1
Carex umbrosa	1
Carlina acaulis	1
Carpinus betulus	1
Carum verticillatum	1
Castanea sativa	1
Centaurea montana	1
Centaurea nigra	1
Centaurea uniflora	1
Centaurium erythraea	1
Cephalanthera damasonium	1

Cephalanthera longifolia	1
Cephalanthera rubra	1
Cephalanthera sp.	0
Cerastium arvense	1
Cerastium fontanum	1
Cerastium fontanum subsp. vulgare	1
Cerastium glomeratum	1
Cerastium sp.	0
Ceratocapnos claviculata	1
Chaerophyllum aureum	1
Chaerophyllum hirsutum	1
Chaerophyllum sp.	0
Chaerophyllum villarsii	1
Chenopodium album	1
Chenopodium bonus-henricus	1
Chrysosplenium alternifolium	1
Chrysosplenium oppositifolium	1
Cicerbita alpina	1
Cicerbita plumieri	1
Circaea alpina	1
Circaea lutetiana	1
Circaea x-intermedia	1
Cirsium arvense	1
Cirsium eriophorum	1
Cirsium oleraceum	1
Cirsium palustre	1
Cirsium sp.	0
Cirsium spinosissimum	1
Cirsium vulgare	1
Cistus salvifolius	1
Clematis alpina	1
Clematis vitalba	1
Clinopodium vulgare	1
Colchicum autumnale	1
Conopodium majus	1
Convallaria majalis	1
Conyza canadensis	1
Corallorhiza trifida	1
Cornus mas	1
Cornus sanguinea	1
Cornus sp.	0
Corylus avellana	1
Cotoneaster nebrodensis	1
Crataegus laevigata	1
Crataegus monogyna	1
Crataegus sp.	0
Crepis biennis	1
Crepis conyzifolia	1
Crepis paludosa	1
Cynoglossum germanicum	1

Cytisus scoparius	1
Cytisus sp.	0
Dactylis glomerata	1
Dactylis sp.	0
Dactylorhiza maculata	1
Danthonia decumbens	1
Danthonia sp.	0
Daphne cneorum	1
Daphne gnidium	1
Daphne laureola	1
Daphne mezereum	1
Daucus carota	1
Deschampsia cespitosa	1
Deschampsia flexuosa	1
Digitalis grandiflora	1
Digitalis lutea	1
Digitalis purpurea	1
Draba sp.	0
Dryopteris affinis	1
Dryopteris affinis subsp. borreri	1
Dryopteris carthusiana	1
Dryopteris dilatata	1
Dryopteris filix-mas	1
Dryopteris remota	1
Dryopteris sp.	0
Elymus caninus	1
Elymus sp.	0
Epilobium angustifolium	1
Epilobium collinum	1
Epilobium hirsutum	1
Epilobium montanum	1
Epilobium obscurum	1
Epilobium sp.	0
Epilobium tetragonum	1
Epipactis atrorubens	1
Epipactis helleborine	1
Epipactis microphylla	1
Epipactis sp.	0
Epipogium aphyllum	1
Equisetum arvense	1
Equisetum palustre	1
Equisetum ramosissimum	1
Equisetum sylvaticum	1
Erica ciliaris	1
Erica cinerea	1
Erica scoparia	1
Erica tetralix	1
Erigeron alpinus	1
Erigeron annuus	1
Euonymus europaeus	1

Euonymus latifolius	1
Eupatorium cannabinum	1
Euphorbia amygdaloides	1
Euphorbia cyparissias	1
Euphorbia dulcis	1
Euphorbia hyberna	1
Euphorbia portlandica	1
Euphorbia serrulata	1
Fagus sylvatica	1
Festuca altissima	1
Festuca curvula	1
Festuca flavescens	1
Festuca gigantea	1
Festuca glauca	1
Festuca heterophylla	1
Festuca ovina	1
Festuca pratensis	1
Festuca rubra	1
Festuca rubra subsp. pruinosa	1
Festuca sp.	0
Festuca tenuifolia	1
Festuca trichophylla	1
Festuca vasconcensis	1
Filipendula ulmaria	1
Fragaria sp.	0
Fragaria vesca	1
Frangula alnus	1
Fraxinus excelsior	1
Fraxinus sp.	0
Galeopsis tetrahit	1
Galium album	1
Galium aparine	1
Galium arenarium	1
Galium aristatum	1
Galium boreale	1
Galium glaucum	1
Galium mollugo	1
Galium odoratum	1
Galium palustre	1
Galium pumilum	1
Galium rotundifolium	1
Galium saxatile	1
Galium sp.	0
Galium sylvaticum	1
Galium uliginosum	1
Galium verum	1
Genista anglica	1
Genista pilosa	1
Gentiana acaulis	1
Gentiana lutea	1

Gentiana purpurea	1
Gentiana verna	1
Gentianella ciliata	1
Geranium columbinum	1
Geranium nodosum	1
Geranium robertianum	1
Geranium sylvaticum	1
Geum montanum	1
Geum rivale	1
Geum sp.	0
Geum urbanum	1
Glechoma hederacea	1
Glechoma hirsuta	1
Glyceria fluitans	1
Glyceria striata	1
Gnaphalium sp.	0
Goodyera repens	1
Gymnocarpium sp.	0
Halimium alyssoides	1
Hedera helix	1
Helictotrichon sedenense	1
Helleborus foetidus	1
Helleborus viridis	1
Helleborus viridis subsp. occidentalis	1
Hepatica nobilis	1
Heracleum sphondylium	1
Hieracium bifidum	1
Hieracium juranum	1
Hieracium laevigatum	1
Hieracium murorum	1
Hieracium pilosella	1
Hieracium prenanthoides	1
Hieracium rapunculoides	1
Hieracium sp.	0
Hieracium umbellatum	1
Hieracium vulgatum	1
Hippocrepis comosa	1
Holcus lanatus	1
Holcus mollis	1
Holcus sp.	0
Homogyne alpina	1
Hordelymus europaeus	1
Hordeum vulgare	1
Humulus lupulus	1
Hyacinthoides non-scripta	1
Hypericum androsaemum	1
Hypericum hirsutum	1
Hypericum humifusum	1
Hypericum maculatum	1
Hypericum montanum	1

Hypericum perforatum	1
Hypericum pulchrum	1
Hypericum richeri	1
Hypericum sp.	0
Hypochoeris maculata	1
Hypochoeris radicata	1
Hypochoeris sp.	0
Ilex aquifolium	1
Impatiens noli-tangere	1
Impatiens sp.	0
Inula conyza	1
Iris foetidissima	1
Isopyrum thalictroides	1
Jasione montana	1
Juglans regia	1
Juncus acutiflorus	1
Juncus bufonius	1
Juncus bulbosus	1
Juncus conglomeratus	1
Juncus effusus	1
Juncus inflexus	1
Juncus sp.	0
Juncus tenuis	1
Juniperus communis subsp. alpina	1
Knautia arvensis	1
Knautia dipsacifolia	1
Knautia dipsacifolia subsp. gracilis	1
Lactuca serriola	1
Lactuca virosa	1
Lamiastrum galeobdolon	1
Lamiastrum sp.	0
Lamium album	1
Lapsana communis	1
Larix decidua	1
Laserpitium halleri	1
Laserpitium siler	1
Laserpitium sp.	0
Lathyrus laevigatus subsp. occidentalis	1
Lathyrus montanus	1
Lathyrus niger	1
Lathyrus pratensis	1
Lathyrus sp.	0
Lathyrus sphaericus	1
Lathyrus tuberosus	1
Lathyrus vernus	1
Leontodon hispidus	1
Leontodon pyrenaicus subsp. helveticus	1
Leontodon sp.	0
Leucanthemum vulgare	1
Ligustrum vulgare	1

Lilium martagon	1
Linaria repens	1
Lithospermum officinale	1
Lobelia urens	1
Lolium perenne	1
Lonicera alpigena	1
Lonicera caerulea	1
Lonicera nigra	1
Lonicera periclymenum	1
Lonicera xylosteum	1
Lotus corniculatus	1
Lotus sp.	0
Lotus uliginosus	1
Lunaria rediviva	1
Luzula campestris	1
Luzula forsteri	1
Luzula luzulina	1
Luzula luzuloides	1
Luzula multiflora	1
Luzula multiflora subsp. congesta	1
Luzula nivea	1
Luzula pilosa	1
Luzula sieberi	1
Luzula sp.	0
Luzula sylvatica	1
Lycopus europaeus	1
Lysimachia nemorum	1
Lysimachia nummularia	1
Lythrum salicaria	1
Maianthemum bifolium	1
Malus sylvestris	1
Marrubium sp.	0
Medicago lupulina	1
Medicago sp.	0
Melampyrum nemorosum	1
Melampyrum pratense	1
Melampyrum sylvaticum	1
Melica nutans	1
Melica uniflora	1
Melittis melissophyllum	1
Mentha aquatica	1
Mentha arvensis	1
Mercurialis perennis	1
Mercurialis sp.	0
Mespilus germanica	1
Milium effusum	1
Minuartia laricifolia	1
Moehringia muscosa	1
Moehringia trinervia	1
Molinia caerulea	1

Molinia caerulea subsp. arundinacea	1
Monotropa hypopitys	1
Mycelis muralis	1
Myosotis alpestris	1
Myosotis scorpioides	1
Myosotis sylvatica	1
Myosoton aquaticum	1
Narcissus bulbocodium	1
Nardus stricta	1
Neottia nidus-avis	1
Odontites verna	1
Orchis purpurea	1
Oreopteris limbosperma	1
Origanum vulgare	1
Ornithogalum pyrenaicum	1
Ornithopus perpusillus	1
Orobanche lutea	1
Orobanche rapum-genistae	1
Orobanche sp.	0
Orthilia secunda	1
Osmunda regalis	1
Osyris alba	1
Oxalis acetosella	1
Oxalis europaea	1
Paris quadrifolia	1
Pastinaca sativa	1
Petasites albus	1
Peucedanum gallicum	1
Peucedanum ostruthium	1
Phalaris arundinacea	1
Phegopteris connectilis	1
Phleum alpinum	1
Phyteuma betonicifolium	1
Phyteuma ovatum	1
Phyteuma sp.	0
Phyteuma spicatum	1
Phytolacca americana	1
Picea abies	1
Picris hieracioides	1
Picris sp.	0
Pimpinella major	1
Pimpinella saxifraga	1
Pinus cembra	1
Pinus pinaster	1
Pinus pinaster subsp. atlantica	1
Pinus sp.	0
Pinus sylvestris	1
Plantago alpina	1
Plantago lanceolata	1
Plantago major	1

Plantago maritima	1
Plantago media	1
Plantago sp.	0
Poa alpina	1
Poa annua	1
Poa bulbosa	1
Poa chaixii	1
Poa compressa	1
Poa nemoralis	1
Poa pratensis	1
Poa sp.	0
Poa supina	1
Poa trivialis	1
Poa trivialis subsp. sylvicola	1
Polygala serpyllifolia	1
Polygonatum multiflorum	1
Polygonatum sp.	0
Polygonatum verticillatum	1
Polygonum bistorta	1
Polygonum mite	1
Polygonum persicaria	1
Polygonum sp.	0
Polypodium vulgare	1
Polystichum aculeatum	1
Polystichum lonchitis	1
Polystichum setiferum	1
Polystichum sp.	0
Populus sp.	0
Populus tremula	1
Potentilla erecta	1
Potentilla grandiflora	1
Potentilla reptans	1
Potentilla sterilis	1
Prenanthes purpurea	1
Primula elatior	1
Primula veris	1
Prunella grandiflora	1
Prunella vulgaris	1
Prunus avium	1
Prunus laurocerasus	1
Prunus padus	1
Prunus serotina	1
Prunus sp.	0
Prunus spinosa	1
Prunus virginiana	1
Pseudarrhenatherum longifolium	1
Pseudorchis albida	1
Pseudotsuga menziesii	1
Pteridium aquilinum	1
Pulmonaria affinis	1

Pulmonaria longifolia	1
Pulmonaria montana	1
Pulmonaria obscura	1
Pulmonaria saccharata	1
Pulsatilla alpina subsp. apiifolia	1
Pyrola media	1
Pyrola minor	1
Pyrus pyraster	1
Quercus ilex	1
Quercus petraea	1
Quercus pubescens	1
Quercus pyrenaica	1
Quercus robur	1
Quercus rubra	1
Quercus sp.	0
Quercus suber	1
Ranunculus aconitifolius	1
Ranunculus acris	1
Ranunculus aduncus	1
Ranunculus auricomus	1
Ranunculus ficaria	1
Ranunculus flammula	1
Ranunculus lanuginosus	1
Ranunculus montanus	1
Ranunculus platanifolius	1
Ranunculus pyrenaeus	1
Ranunculus repens	1
Ranunculus serpens subsp. nemorosus	1
Ranunculus sp.	0
Rhamnus catharticus	1
Rhododendron ferrugineum	1
Ribes alpinum	1
Ribes rubrum	1
Ribes uva-crispa	1
Rosa arvensis	1
Rosa canina	1
Rosa pendulina	1
Rosa pimpinellifolia	1
Rosa villosa	1
Rubia peregrina	1
Rubus caesius	1
Rubus canescens	1
Rubus fruticosus	1
Rubus idaeus	1
Rubus questieri	1
Rubus saxatilis	1
Rubus sp.	0
Rubus ulmifolius	1
Rubus vestitus	1
Rumex acetosa	1

Rumex acetosella	1
Rumex alpestris	1
Rumex alpinus	1
Rumex obtusifolius	1
Rumex sanguineus	1
Rumex scutatus	1
Rumex sp.	0
Ruscus aculeatus	1
Salix atrocinerea	1
Salix caprea	1
Salix cinerea	1
Salix elaeagnos	1
Salix repens	1
Salix sp.	0
Sambucus ebulus	1
Sambucus nigra	1
Sambucus racemosa	1
Sambucus sp.	0
Sanguisorba minor	1
Sanicula europaea	1
Saxifraga cuneifolia subsp. robusta	1
Saxifraga granulata	1
Saxifraga rotundifolia	1
Scilla bifolia	1
Scirpus sylvaticus	1
Scorzonera humilis	1
Scrophularia alpestris	1
Scrophularia nodosa	1
Scutellaria minor	1
Scutellaria sp.	0
Sedum anacampseros	1
Sedum montanum	1
Sempervivum arachnoideum	1
Sempervivum tectorum	1
Senecio adonidifolius	1
Senecio jacobaea	1
Senecio nemorensis subsp. fuchsii	1
Senecio sp.	0
Senecio sylvaticus	1
Senecio viscosus	1
Senecio vulgaris	1
Serratula tinctoria	1
Seseli montanum	1
Sesleria albicans	1
Setaria sp.	0
Silene dioica	1
Silene nutans	1
Silene rupestris	1
Silene vulgaris	1
Simethis planifolia	1

Sison amomum	1
Sisymbrium orientale	1
Solanum dulcamara	1
Solanum nigrum	1
Soldanella alpina	1
Solidago canadensis	1
Solidago gigantea	1
Solidago sp.	0
Solidago virgaurea	1
Sonchus arvensis	1
Sonchus asper	1
Sonchus oleraceus	1
Sonchus sp.	0
Sorbus aria	1
Sorbus aucuparia	1
Sorbus domestica	1
Sorbus sp.	0
Sorbus torminalis	1
Stachys alpina	1
Stachys officinalis	1
Stachys sylvatica	1
Stellaria graminea	1
Stellaria holostea	1
Stellaria media	1
Stellaria nemorum	1
Stellaria uliginosa	1
Succisa pratensis	1
Tamus communis	1
Taraxacum officinale	1
Taraxacum sp.	0
Taxus baccata	1
Teucrium scorodonia	1
Thalictrum aquilegiifolium	1
Thalictrum sp.	0
Thesium alpinum	1
Thlaspi alpestre	1
Tilia cordata	1
Tilia platyphyllos	1
Tilia platyphyllos subsp. cordifolia	1
Torilis japonica	1
Tragopogon pratensis	1
Trifolium alpestre	1
Trifolium alpinum	1
Trifolium badium	1
Trifolium medium	1
Trifolium pratense	1
Trifolium repens	1
Trifolium sp.	0
Trisetum flavescens	1
Trochiscanthes nodiflora	1

Trollius europaeus	1
Tussilago farfara	1
Ulex europaeus	1
Ulex minor	1
Ulmus glabra	1
Ulmus minor	1
Urtica dioica	1
Vaccinium myrtillus	1
Vaccinium vitis-idaea	1
Valeriana montana	1
Valeriana officinalis	1
Valeriana officinalis subsp. sambucifolia	1
Valeriana tripteris	1
Veratrum album	1
Verbascum lychnitis	1
Verbascum nigrum	1
Verbascum sinuatum	1
Verbascum thapsus	1
Veronica anagallis-aquatica	1
Veronica beccabunga	1
Veronica chamaedrys	1
Veronica hederifolia	1
Veronica hederifolia subsp. lucorum	1
Veronica montana	1
Veronica officinalis	1
Veronica serpyllifolia	1
Veronica serpyllifolia subsp. humifusa	1
Veronica sp.	0
Veronica urticifolia	1
Viburnum lantana	1
Viburnum opulus	1
Vicia cracca	1
Vicia disperma	1
Vicia hirsuta	1
Vicia pisiformis	1
Vicia sativa	1
Vicia sativa subsp. nigra	1
Vicia sepium	1
Vicia sp.	0
Vicia sylvatica	1
Vicia tetrasperma	1
Vinca minor	1
Vincetoxicum hirundinaria subsp. intermedium	1
Viola biflora	1
Viola canina	1
Viola hirta	1
Viola mirabilis	1
Viola odorata	1
Viola reichenbachiana	1
Viola riviniana	1

Viola sp.	0
Viola tricolor	1

(Intercept)	Age_1995	Disturbanc	Years	Stand_Typ	Exclosure e	Cumulated	Cumulated	Stand basa
0.838	0.145	-0.115	0.058			-0.17		0.216
0.838	0.152	-0.113	0.059			-0.167	-0.042	0.207
0.811	0.16	-0.113	0.055	+		-0.165		0.208
0.83	0.145	-0.115	0.058		+	-0.17		0.216
0.805	0.17	-0.11	0.055	+		-0.161	-0.045	0.196
0.838	0.121	-0.087				-0.114		0.195
0.83	0.152	-0.113	0.059		+	-0.167	-0.042	0.207
0.838	0.127	-0.085				-0.111	-0.04	0.185
0.797	0.145	-0.087		+		-0.111		0.184
0.803	0.16	-0.113	0.055	+	+	-0.165		0.208
0.792	0.154	-0.084		+		-0.107	-0.044	0.172
0.797	0.17	-0.11	0.055	+	+	-0.161	-0.045	0.196
0.83	0.121	-0.087			+	-0.114		0.195
0.83	0.127	-0.085			+	-0.111	-0.04	0.185
0.789	0.145	-0.087		+	+	-0.111		0.184
0.784	0.154	-0.084		+	+	-0.107	-0.044	0.172
0.837		-0.084				-0.09		0.185
0.837		-0.099	0.033			-0.118		0.196
0.877		-0.104	0.041	+		-0.133		0.211
0.862		-0.085		+		-0.094		0.193

Baseline te	df	logLik	AICc	delta	weight	R2_marg	R2_cond
0.766	11	-2304.28	4630.707	0	0.214	0.329	0.549
0.757	12	-2303.63	4631.446	0.738	0.148	0.331	0.547
0.778	12	-2304.07	4632.328	1.621	0.095	0.33	0.549
0.766	12	-2304.25	4632.681	1.974	0.08	0.329	0.549
0.77	13	-2303.34	4632.881	2.173	0.072	0.332	0.547
0.754	10	-2306.41	4632.955	2.248	0.07	0.325	0.543
0.757	13	-2303.61	4633.42	2.713	0.055	0.331	0.547
0.745	11	-2305.83	4633.804	3.097	0.046	0.326	0.541
0.773	11	-2305.95	4634.042	3.335	0.04	0.327	0.544
0.778	13	-2304.05	4634.305	3.597	0.035	0.33	0.549
0.765	12	-2305.22	4634.617	3.909	0.03	0.329	0.541
0.77	14	-2303.31	4634.858	4.15	0.027	0.332	0.547
0.754	11	-2306.39	4634.927	4.22	0.026	0.325	0.543
0.745	12	-2305.8	4635.777	5.07	0.017	0.326	0.541
0.773	12	-2305.92	4636.016	5.309	0.015	0.327	0.544
0.765	13	-2305.19	4636.592	5.884	0.011	0.329	0.541
0.698	9	-2310.65	4639.41	8.703	0.003	0.32	0.545
0.698	10	-2309.94	4640.008	9.301	0.002	0.322	0.548
0.691	11	-2309.39	4640.939	10.232	0.001	0.322	0.548
0.694	10	-2310.43	4640.978	10.271	0.001	0.32	0.545

References	Years	Journal	Methods to compute the CTI
Bertrand et al.	2011	Nature	CTI reconstructed using a combination of weighted averaging partial least squares and Breiman's random forest with transfer function
Brice et al.	2019	Global Ecology and Biogeography	CTI computed with the average of species temperature distributions (i.e. Wordclim) based on tree occurrence data (Forest inventory databases of eastern North America)
Cheung et al.	2013	Nature	CTI based on the average of temperature preferences of marine fishes and invertebrates in fisheries catch
De Frenne et al.	2013	PNAS	CTI computed with temperature preference distributions of species (during growing season April to September) in permanent or semipermanent plots
Devictor et al.	2008	PNAS	CTI calculated as the average of species thermal preferences
Devictor et al.	2012	Nature Climate Change	CTI calculated as the average of species thermal preferences
Devictor et al.	2012	Nature Climate Change	CTI calculated as the average of species thermal preferences
Fadrique et al.	2018	Nature	CTI calculated as the average of species thermal preferences
Flanagan et al.	2019	Ecography	CTI calculated as the average of species thermal preferences
Fourcade et al.	2018	Biodiversity and Conservation	CTI calculated as the average of species thermal preferences
Gotfried et al.	2012	Nature Climate Change	Temperature index with ecological indicator
Haase et al.	2019	Science of the Total Environment	CTI calculated as the average of species thermal preferences
Lindström et al.	2013	Ecography	CTI calculated as the average of species thermal preferences

Savage et al.	2015	Ecography	CTI calculated as the average of species thermal preferences
Elmendorf et al.	2015	PNAS	CTI calculated as the average of species thermal preferences ; Repeated sampling of historical studies and warming experiments
Duque et al.	2015	PNAS	CTI calculated as the average of species thermal preferences
Zellweger et al.	2020	Science	CTI calculated as the average of species thermal preferences

Methods to compute the velocity of changes	Period
Differences between CTI from between 1965-1986 and 1987-2008 periods	1965-1986 and 1987-2008
Comparison between historical and contemporary periods	1970 - 2016
Slope of linear regression	1970 - 2006
Comparison between historical and contemporary periods	depending on forest plots and regions; overall, from 1940 (minimum) to 2009 (maximum)
Slope of linear regression	1989 - 2006
Slope of linear regression	1990 - 2008
Slope of linear regression	1990 - 2008
Slope of linear regression	2000 - 2015
Slope of linear regression	1990 - 2014
Comparison between historical and contemporary periods	1960 - 2011
Comparison between historical and contemporary periods	2001 - 2008
Slope of linear regression	1990 - 2014
Slope of linear regression	1975 - 2009

Comparison between historical and contemporary periods	1970 - 2012
Slope of linear regression	1970 - 2012
Rates calculated as the annualized change in the CTI values for each plot over the entire census period	2006-2014
Comparison between baseline surveys and resurveys	depending on forest plots and regions; overall, from 1934 (minimum) to 2017 (maximum) ; median time interval between two surveys of 38 years

Taxonomic groups	Regions	Thermophilization rates
Forest understorey vegetation	France	Δ0.02°C and Δ0.54°C between 1965-1986 and 1987-2008 in lowland and highland, respectively.
Tree communities	Canada, Québec	0.03°C / decade
Marine fishes and invertebrates	Global	0.19°C / decade
Forest understorey vegetation	29 regions of Europe and North America	0.041°C / decade
Birds	France	0.044°C / decade
Birds	Europe	0.044°C / decade
Butterflies	Europe	0.051°C / decade
palms, tree ferns and lianas (Trees (including	The Andes (Peru, Colombia, Argentina, Ecuador)	0.066°C / decade
Marine fishes and invertebrates	Northeast U.S. continental shelf	in fall: 0.25°C / decade; in spring: 0.38°C / decade
Bumblebees	Norway	0.14°C / decade
Mountain vegetation	Europe	-
Stream invertebrate communities	Central Europe	0.22°C / decade (abundance data); 0.15°C / decade (occurrence data)
Birds	Norway	0.031°C / decade (Old monitoring scheme); 0.096°C / decade (New monitoring scheme)

Forest understorey vegetation	Canada, Québec	0.05° C / decade
Tundra vegetation	Canada, Québec	0.199° C / decade
Tree communities	Northern tropical Andes	adult trees: 0.11°C / decade; juvenile trees: 0.27°C / decade
Forest understorey vegetation	Europe	0.01°C / decade